UNIVERSITY OF TRENTO - Italy
Department of Civil, Environmental and Mechanical Engineering

Doctoral School in Civil, Environmental and Mechanical Engineering
Topic 2. Mechanics, Materials, Chemistry and Energy - XXXI cycle 2016/2018

Doctoral Thesis - April 2019

Elena Bee

Heat pump and photovoltaic systems in residential applications

Performance, potential, and control of the system

Supervisor
Prof. Paolo Baggio, University of Trento
Co-supervisor
Dr. Alessandro Prada, University of Trento

ISBN (paper): ..... ; ISBN (online): .....

University of Trento
Doctoral School in Civil, Environmental and Mechanical Engineering
http://web.unitn.it/en/dricam
Via Mesiano 77, I-38123 Trento
Tel. +39 0461 282670 / 2611 - *dicamphd@unitn.it*

Abstract

Air-source heat pumps coupled with photovoltaic systems are going to be a more and more promising technology, as its widespread application in residential houses will help achieving the decarbonisation of the building sector, which is strongly promoted by the European Union.
The aspects that inspire confidence for this solution are that: i) the average quality of heat pumps has recently improved; ii) new and renovated buildings, with well insulated envelopes, are more suitable for low-temperature heating systems; iii) photovoltaic modules price is significantly decreased and still shows a diminishing trend; iv) the share of the electricity production from renewable sources is progressively increasing, making the use of electricity more ecologically favourable and v) heat pump and photovoltaic systems can make the residential sector flexible and ready to face the changes in the electricity system.
The aim of this thesis is to analyse the manifold relationships between the building, the HVAC system and the boundary conditions, as well as the interaction of this system with the electricity grid. The work is almost entirely based on the dynamic simulation, which is performed by using more or less detailed models, depending on the objective of the single study. The heat pump is a crucial element, since its behaviour is influenced by many factors. Therefore, particular attention is pointed toward the modelling of this component and its control. The general approach mainly adopted is the comparison between a reference system, defined case by case, and other similar scenarios in which one or more variations are introduced. Since different aspects are investigated, the variations can concern either the system component (building and HVAC system), the boundary conditions or the control strategy. In particular, one of the studies provide an extensive analysis on how the climate impacts the behaviour of the system, involving nine European cities in a wide range of latitude. The role of the thermal storage (water tank and building thermal mass) is also studied, showing that its potential is exploited only when it is properly controlled. The last part of the thesis focuses on the system control, which influences the system performance more than expected. Despite this, the benefits of applying the proposed smart control strategies are not as great as those deriving from

the addition of the electrical storage, in a system in which only the thermal storage is present. Even better results can be obtained by applying control strategies that also manage the battery charging/discharging. A general conclusion is that rule-based control strategies would be cheap and effective; however, they require a tailored implementation and their development for the mass-market is not easy.

Table of Contents

List of Tables

List of Figures

Figure **Page**

Acronyms

ASHP	air-source heat pump
AWHP	air-to-water heat pump
COP	coefficient of performance
DHW	domestic hot water
EER	energy efficiency ratio
FC	frequency controlled HP model
FE	final energy
FSCO	fractional state of charge
HP	heat pump
HVAC	heating, ventilation, and air conditioning
IC	initial costs
NCOE	net cost of electricity
NN	neural network
NPV	net present value
nZEB	nearly zero-energy buildings
PEF	primary energy factor
PI	proportionally integrative
PV	photovoltaic
RTP	real-time price
SC	self-consumption
SCOP	seasonal coefficient of performance
SEER	seasonal energy efficiency ratio
SF	solar fraction
SH	space heating
SP	set point
SPF	seasonal performance factor
SSr	self-sufficiency ratio
TC	temperature controlled HP model
TMY	typical meteorological year
TOU	time-of-use
TRY	test reference year

CHAPTER 1

Introduction

1.1 Background and motivation

The 2010 Energy Performance of Buildings Directive (European Union, 2010) and the 2012 Energy Efficiency Directive (European Union, 2012) are the main legislative instruments that the EU introduced in order to improve the energy performance of buildings. The former, which introduces the concept of nearly zero-energy buildings (nZEB) and requires to cover a share of the energy need with renewable energy sources, has been revised in May 2018. Some additional contents in the new version state that EU countries will have to establish stronger long-term renovation strategies, aiming at decarbonising the national building stocks by 2050, and that smart tech-

nologies will be further promoted, for instance through requirements on the installation of building automation and control systems. Heat pumps (HPs) are acknowledged as a technology that uses renewable energy (European Commission, 2009), which also has the potential to reduce greenhouse gas emissions and to increase energy efficiency. Despite their low share in the European heating market, they have an increasingly growing trend in the number of sales (+20% in two years 2017-2018 in Europe, mainly driven by the growth in air-source HPs (ASHPs), (International Energy Agency, 2019)). Also according to the European Heat Pump Market and Statistics Report 2015 (European Heat Pump Agency, 2015), air is and will remain the dominant energy source for heat pumps installed across Europe (heating units). Typically, when an electric-driven ASHP is operating in the heating mode, it uses electricity to transfer heat from the air to a higher temperature fluid (air or water), by means of a vapour compression cycle. The primary energy use due to the HP operation, and consequently its environmental impact, depends, basically, on the value of the coefficient of performance (COP) in the actual operating conditions and on the efficiency of the electrical generation and distribution system. With respect to the former aspect, there is still room for improvement, both in terms of research and of system application (heat pump manufacturers and system designers), despite a significant progress in recent years. The adoption of inverter-driven compressors improves the COP of typical commercial products (Chua et al., 2010), especially at part load operations. Photovoltaic (PV) systems in combination with ASHPs can also reduce the CO_2 emission (Luthander et al., 2015; Williams et al., 2012). Besides, also the emissions due to the share of electricity drawn from the grid are supposed to drop on a long-term perspective, in order to meet the decarbonisation goals.

Ultimately, when designed properly, heat pump is an energy-efficient technology that reduces greenhouse gas emissions especially when it is combined with a PV system (Facci et al., 2018; Luthander et al., 2015; Williams et al., 2012). Therefore, it contributes to the long-term goal of achieving a sustainable society [1].

As for the competitiveness on the market, the energy prices, which vary widely from one country to another, and each country's energy mix play a key role in determining the economical convenience of adopting HPs for heating and cooling application in the residential buildings. However, the market penetration of this technology is also influenced by the tradition of the building sector, the knowledge of its potential, and the condition of existing buildings. In countries where the majority of the electricity production comes mainly from fossil fuels and/or the electricity prices have limited competitiveness (*e.g.*, Italy[2]), the growth of the HP market can be encouraged by other means, such as, research and development, political incentives, requirements for specific minimum levels of energy efficiency, and the dissemination of knowledge. Besides the above mentioned aspects, the climate, which also shows a large variability across Europe, is another factor that contributes to the heterogeneity of the residential heating and cooling sector in Europe. However, HP systems coupled with PV are becoming a promising solution in the residential sector. As mentioned above, one of the reason for that is the need for decarbonisation of the building sector, clearly promoted by the EU. Other aspects that foster this technology are that:

[1] EHPA calculated the heat-pump renewable energy potential in Europe by taking Norway as reference country and found that many countries can (over-)achieve the 2020 targets if they uncap the full heat pump potential, (European Heat Pump Agency, 2018).

[2] In Italy, the renewable share (hydro, wind, geothermal, and photovoltaic) of the electricity production mix was 34% in 2018 (Terna, 2019 - January 2019 Monthly report on the Electricity System) and it has an electricity prices for household consumers (taxes included) higher than the EU-28 mean in the first half 2018 (eurostat, 2018).

- HP units have been improved during the last years, especially at the part load operation;
- new and renovated building with well insulated envelope are more suitable for low-temperature heating system, such as HPs;
- PV modules price is significantly decreased (both high efficiency and mainstream modules) and still shows a diminishing trend (PV Magazine, 2019);
- the share of the electricity production from renewable sources is progressively increasing, making the use of electricity more ecologically favourable.

Besides, the analysed system offers the possibility to decouple energy consumption from energy demand by using a different kind of storage techniques and by means of demand side management. This brings flexibility to the system and allows us to frame it in smart grid context. Considering also the less attractive PV feed-in-tariffs with respect to some years ago, maximizing self-consumption becomes a primary objective, to be pursued by means of both a proper design (sizing) and a proper control of the system. In fact, the combination of heat pumps and PV is not always enough to ensure good self-consumption levels. Boosting the self-consumption is a central aspect of this thesis.

Several studies on this subject have been presented in the last decade, but it seems that, when it comes to installations, the problem is still not sufficiently considered. The typical situation (in buildings with both a heat pump and a PV system) is that the self-consumption follows the natural matching between energy demand and energy availability (PV production). The industry gap may be due to the poor dissemination or to the fact that

it is not clear to what extent the self-consumption can be increased. It also worth considering that, on the one hand, analysing the problem in a specific context is not sufficient to give an answer and, on the other hand, it is not easy to include the multitude of possible scenarios.
Many authors have recently studied the HP systems flexibility (Fischer and Madani, 2017; Fischer et al., 2015; Luthander et al., 2015; Schibuola et al., 2015; Thygesen and Karlsson, 2016; Masy et al., 2015; Patteeuw et al., 2016; Pallonetto et al., 2016; Arteconi et al., 2013; Péan et al., 2019; Arteconi et al., 2019; Junker et al., 2018; Clauß et al., 2019), thus confirming the relevance and the good timing of the topic. However, as also stated by (Beck et al., 2017) the studies on the ability of heat pump systems to increase self-consumption of PV-electricity are still limited, thus posing the need for further analyses.

1.2 Thesis structure

Below, an overview of the structure of this thesis is provided.

Chapter 1 (current chapter) defines the motivation and research objectives and summarizes the contents of this work.

Chapter 2 describes the overall methodology, the system modelling, and the assumptions. Moreover, the system boundaries and performance indicators are defined.

Chapter 3, investigates various methods and calculation procedures to evaluate the performance of the HP at part load operation and the impact of the possible choices about the method to be applied. Moreover, the in-

fluence of different choices on the system design is shown.

Chapter 4 analyses the impact of the climate on the system and in particular on its potential in terms of self-consumption of the electricity produced on-site and the self-sufficiency with respect to the heating and cooling needs of a single family house.

Chapter 5 involves various studies which are all related to the enhanced control of the system, aiming at increasing the self-consumption, the self-sufficiency or at reducing the energy use and the annual cost.

Chapter 6 concludes this work and it is aimed at providing an overview of the performed analyses, summarising the key aspects according to the author's opinion, and highlighting how this doctoral thesis contributes to the knowledge in this scientific field.

1.3 Research output

This doctoral thesis is mainly based on the research studies and activities published in the following peer-reviewed papers. However, in the last part of the thesis, further considerations and results are included.

1.3.1 Publications discussed in this work

Paper 1 *Variable-Speed Air-to-Water Heat Pumps for Residential Buildings: Evaluation of the Performance in Northern Italian Climate*. E. Bee, A. Prada, P. Baggio. Proceedings of 12th REHVA world congress (Aalborg, Denmark, 2016).

Paper 2 *Evaluation of the Seasonal COP of Air-to-Water Heat Pumps with Inverter in Different Italian Climates*. E. Bee, A. Prada, P. Baggio. 34th AiCARR Congress 2016 (Bologna, Italy, 2016).

Paper 3 *On the Influence of Storage Size and Management on the Consumption of Air Source Heat Pumps in High Performance Buildings*. E. Bee, A. Prada, P. Baggio. BSA Conference 2017 (Bolzano, Italy, 2017).

Paper 4 *Smart control strategy for PV and heat pump system utilizing thermal and electrical storage and forecast services*. E. Psimopoulos, E. Bee, R. Luthander, C. Bales. Solar World Congress 2017 (Abu Dhabi, United Arab Emirates, 2017).

Paper 5 *On the Optimal Mix between Lead-Acid Battery and Thermal Storage Tank for PV and Heat Pump Systems in High Performance Buildings*. Prada A., Bee E., Grigiante M., Baggio P.(2017). Energy Procedia 140,423-433.

Paper 6 *Rule Based Control Strategies of Thermal Storage in Residential Heating Systems with Air-Source Heat Pump and Photovoltaic Panels*. Bee E., Prada A., Baggio P. Proceedings of 2018 Purdue Conferences (West Lafayette (IN), United States, 2018).

Paper 7 *Air Source Heat Pump Systems: Control Strategy Based on the Knowledge of the Time Evolution of the Electricity Price in the Italian Context*. Bee E., Prada A., Baggio P. Proceedings of 2018 Purdue Conferences (West Lafayette (IN), United States, 2018).

Paper 8 *Air-Source Heat Pump and Photovoltaic Systems for Residential Heating and Cooling: Potential of Self-Consumption in Different European Climates*. Bee E., Prada A., Baggio P., Psimopoulos E. (2018). Building Simulation https://doi.org/10.1007/s12273-018-0501-5.

Paper 9 *Techno-Economic Analysis of Control Algorithms for a PV and Heat Pump system for Residential Buildings*. Psimopoulos E., Bee E., Widén J., Bales C. To appear in Applied Energy.

Paper 10 *Demand-Side Management of Air-Source Heat Pump and PV for Heating Applications in the Italian Context*. Bee E., Prada A., Baggio P. (2018) Environments 5(12), 132– Special Issue "Smart Energy Management for a Sustainable Built Environment."
https://doi.org/10.3390/environments5120132

1.3.2 Additional publications

Hereafter, other related publications that are not included in this thesis are listed.

Paper 11 *Inverter-Driven Heat Pumps for Space Heating: Comparisons of Air-to-Water and Air-to-Air Units*. E. Bee, A. Prada, P. Baggio. Building Simulation 2017 (San Francisco (CA), United States, 2017).

Paper 12 *Optimization of Air-Source Heat Pump Systems over the Heating Season through the Use of Renewable Energy*. E. Bee, A. Prada, P. Baggio. Proceedings of 2016 Purdue Conferences (West Lafayette (IN), United States, 2016).

CHAPTER 2

System model and KPIs

The operation of heat pumps is strongly dependent on both the outside temperature and on the load. In order to correctly evaluate the performance, the specific applications of the unit need to be properly taken into account. The actual seasonal coefficient of performance (SCOP) is usually different from the one declared in the manufacturers' data sheets and also from that evaluated with the calculation procedure defined in the Italian standard UNI TS 11300-4 ("bin method") (UNI, 2016*b*), which is based on the European standard EN 14825 (European Commission, 2016). Moreover, the HP performance is affected by the following:

- the defrosting cycles losses;

- the losses due to the transient after the switch on;
- in variable speed units, the COP variation at part load conditions.

In particular, neglecting the COP variation at part load operation of variable speed units typically leads to underrate the performance. However, the information on how the COP varies is rarely declared by the manufacturers and it is thus difficult to correctly simulate a specific market product. According to the Italian technical specification UNI TS 11300-4 (which is based on the standard EN 14825), the COP at part load conditions for variable capacity can be evaluated by multiplying it by a correction factor, f_{corr}, that depends on the capacity ratio, CR, as follows:

$$COP_{PL} = f_{corr}\,(CR) \cdot COP \tag{2.1}$$

The correction factor, if not otherwise specified, is equal to 1 for CR larger than the minimum modulation capacity (or larger than 0.5, if the minimum modulation capacity is not declared) and it follows the degradation function of fixed-speed units as shown below for lower values of CR:

$$f_{corr} = \frac{CR}{C_c \cdot CR + (1 - C_c)} \tag{2.2}$$

where C_c, if not declared, is equal to 0.9. These formulae are not particularly representative of the last generation products, the performance of which at part load operation is typically better. Therefore, the assumptions of the legislation are cautelative. It is also worthwhile considering that the legislation was published in 2012, when the market of HPs was facing a transition from fixed-speed to variable-speed units. Another legislation, the EN 15316-4-2:2008 (European Commission, 2008), which is even older, cites as follows: "*Stepwise or continuously controlled variable capacity units, e.g. by means of an inverter for electrically-driven heat pumps*

[...], may have a better efficiency at part load. On the one hand, this may already be reflected in the full load values according to standard testing, e.g. EN 14511 for electrically-driven heat pumps, on the other hand, part load COP may be more efficient." This statement denotes the lack of certainty on the performance of the market products at that time.
Since one of the objective of this thesis work is to investigate, by means of dynamic simulations, the potential of the variable-speed air-source heat pump systems in real operation scenarios (*i.e.*, coupled with buildings), a dynamic model of the unit is needed.

2.1 Modelling the HP

In general, HP modelling can be approached by means of either a physical model of the fluid cycle (*i.e.*, by modelling the heat exchangers, the compressor, and the various components) or a model based on the performance map, which is a sort of a black box with respect to the refrigerant thermodynamic cycle and it only calculates the outlet temperature of the source and sink fluids and the power absorbed by the compressor (*i.e.*, the interaction of the unit with the external environment). The former approach is typically more demanding from the computational point of view, and it is therefore not well suited to the dynamic simulation of the whole system (building and Heating, Ventilation, and Air Conditioning, HVAC). Models based on the performance map have been chosen in the majority of the studies involving the dynamic simulation of building systems with HPs.
As outlined in the introduction, the most extensively used software in this thesis is TRNSYS (Transient System Simulation Tool). The available TRNSYS models in the standard and TESS (Thermal Energy System Specialists) libraries are capable to model air-source HPs with a constant speed

compressor. Recently, HPs with variable speed compressors have also entered the market; the compressor speeds up and slows down to provide more or less heating and cooling as needed by the building. Hence, a model for variable speed heat pumps has been coded, and the structure of the code is outlined in the following.
The first version of the model is controlled by a set temperature of the fluid exiting the machine at the sink side; therefore, this version will be denoted by TC (Temperature Controlled) model. The second version of the model is controlled by an input signal representing the frequency of the compressor and it is called FC (Frequency Controlled) model. Both versions are developed in Fortran, as the majority of the TRNSYS components and the TRNSYS engine itself are written in this language, and compiled into a dynamic link library (DLL) for Windows operating systems.

2.1.1 TC model

The procedure related to the Temperature Controlled model is as follows:

1. The first step to be performed in the code is the operation mode check (heating or cooling) based on an input signal. Hereby, only the heating mode will be explained, since the cooling mode is symmetric.

2. The ideal required thermal power is computed as follows:

$$P_{req} = m \cdot c_w \cdot (T_{w,set} - T_{w,in}) \tag{2.3}$$

   where m, $T_{w,set}$, and $T_{w,in}$ are input variables (*i.e.*, they can change at each time step) representing respectively the mass flow, set temperature for the supply water; and the inlet water temperature; c_w is the specific heat of the water.

3. Based on the above, the capacity ratio is determined as the ratio $CR = P_{req}/P_{nom}$. This ratio can be lower or higher than 1.

4. Depending on the value of CR, three situations can occur:

   - $CR > 1$: the HP is working at nominal speed with the nominal COP; the temperature required by the control system is too high for this machine. The heat pump operates at the maximum speed and it will transfer to the water the maximum heating power that it is able to provide.
   - $CR_{min} < CR < 1$: the HP is working at part load with the corrected COP as declared in the manufacturer's data. The outlet water temperature is exactly the desired one (*i.e.*, $T_{w,set}$). The COP is corrected by interpolating the manufacturer's data or, alternatively, by using a parametric curve, which is defined by means of 2 parameters (see Figure 3.8).
   - $CR_{lim} < CR < CR_{min}$: the HP is working in on/off mode because CR is below the modulating capacity limit; the COP is significantly degraded, according to the degradation function in EN14825 for variable speed units under their minimum modulation capacity. In this operation mode, the HP still provides some power in order to supply water at the $T_{w,set}$ temperature, but the COP is low.
   - $CR < CR_{lim}$: this interval is introduced to avoid numerical problems which might arise due to very low values of COP, with consequent unrealistic electric consumption values. The following behaviour can be highlighted for f_{corr}:

$$\lim_{CR \to 0} f_{corr}\left(CR\right) = 0$$

The function application has therefore a lower limit, CR_{lim}, below which the machine is off. The supply water temperature is set equal to the inlet water temperature, regardless the set temperature; CR_{min} and CR_{lim} are parameters defined by the user.

5. Regardless of the case that occurs, step 4 outcome is an effective thermal power, $P_{th,eff}$, and a COP value. The outlet water temperature is therefore computed as:

$$T_{w,out} = T_{w,in} + \frac{P_{th,eff}}{m \cdot c_w} \tag{2.4}$$

2.1.2 FC model

The TC model has been used for different studies presented in this thesis. Although this model is capable to simulate the behaviour of variable speed HPs, an issue arose when advanced control algorithms had to be implemented. Specifically, it was noticed that the application of specific control strategies requires to directly control the machine operation. In real applications, this is carried out by interfacing the control algorithm output signal with the unit's electronic shield. Since the final control action on the heat pump is to define the compressor speed, it is preferable to have a HP model that takes such variable as an input. The whole control strategy is therefore implemented externally to the HP model. This approach is also more similar to what happens in real HPs. Another issue on HP modelling is that a trade-off has to be found between versatility and specificity of the model. On the one hand, there is the need for a versatile model suitable for a range of products of different manufacturers, with configurable parametric features. On the other hand, in order to be able to simulate the operation of a specific machine, it would be necessary to either know

the internal control mechanism or make some hypothesis on it. Having the control strategy as an external subroutine also brings the advantage that it can be changed without compiling and linking the dynamic link library each time. As mentioned above, gathering information from manufacturers on the HP performance at part load condition is not easy. However it is even less likely that the manufacturer provides information on the control algorithm and on how the compressor reacts to changing inlet conditions. The steps of the FC model are described below.

1. See step 1 in the TC model.

2. Based on the desired input frequency (f) and on the nominal compressor frequency (f_{nom}), the capacity ratio (CR) is determined as:

$$CR = \frac{f - f_{nom}}{f_{nom}} \tag{2.5}$$

   This ratio can be lower or higher than 1. Its minimum and maximum values are $CR_{min} = (f_{min} - f_{nom})/f_{nom}$ and $CR_{max} = (f_{max} - f_{nom})/f_{nom}$, where f_{min} and f_{max} are parameters of the model representing, respectively, the minimum and maximum modulation frequencies.

3. Three situations can occur:

   - $CR > CR_{max}$: unlike the TC model, this situation should not occur, but, if it is the case, the CR value is fixed to CR_{max}. The HP operates at the maximum speed and it will transfer to the water the maximum heating power that it is able to provide.
   - $CR_{min} \leq CR \leq CR_{max}$: based on the water temperature supplied at the previous time step and the outdoor air temperature,

the thermal power and the COP corresponding to the nominal frequency are calculated by interpolating the performance map. The COP is then corrected by means of f_{corr}.

- $CR < CR_{min}$: the HP is turned off, regardless of the input control signal. Both the thermal power and the COP are set to 0.

4. Knowing the effective thermal power and the effective COP, the outlet water temperature and the absorbed power are calculated as follows:

$$\begin{aligned} T_{w,out} &= T_{w,in} + \frac{P_{th,eff}}{m \cdot c_w} \\ P_{el} &= \frac{P_{th,eff}}{COP_{eff}} \end{aligned}$$

where P_{el} is the absorbed electric power.

The FC model is designed to operate with small time steps (*i.e.*, 1 minute).

2.1.3 Exhaust air heat-pump model

In the Swedish context, exhaust-air HPs constitute the majority of heat pumps applications in dwellings; therefore, in this scenario, a different model is used. The considered model represents a market leading variable-speed exhaust-air compact heat pump for both space heating (SH) and domestic hot water (DHW). The HP is modelled by means of TRNSYS type 581; this is a multidimensional interpolator in which the input variables are the inlet air temperature, the inlet water temperature, and the compressor speed, while the output variables are the heating rate capacity and the compressor power input. TRNSYS type 581 reads a HP performance map that is derived from detailed steady state measurement data provided by the manufacturer for the full range of temperatures and compressor speed

values. The performance takes into account the energy required for the defrosting cycles of the evaporator. A heating curve with a design supply temperature of 38°C for an ambient temperature of −15°C is applied and the compressor speed is controlled according to this curve. The controller also uses a proportionally integrative (PI) compensatory algorithm, based on the SH supply temperature.

2.2 Modelling the overall system

In this section, the main components used in the TRNSYS simulation suite are described. In particular, the focus is on the models used for the water storage tank and the emission sub-system (*i.e.*, the heat exchange with the building zones). Then, the modelling of the boundary conditions is outlined, in particular referring to occupancy, DHW tapping profiles, weather variables, and electricity prices.

2.2.1 Water storage tank

Most of the analyses reported in this thesis involve a water storage tank, for which a detailed built-in TRNSYS model (type 60) was exploited. This component models a stratified fluid storage tank with optional internal heaters and optional internal heat exchangers. The tank volume consists of a variable number of fully-mixed equal volume segments. Since this model is suitable for a wide range of configurations, it is used for two different application:

- a buffer tank for SH water (radiant-floor or fancoils) with two inlets and two outlets;

- a storage tank for DHW, with an internal heat exchanger, one inlet and one outlet, and an auxiliary back-up heater.

Both of the tanks are shaped as a vertical cylinder and the thermal losses through the tank envelope are taken into account by means of a total heat transfer coefficient (U), which, based on the average market product, is set to 0.35 W/m^{2}K. Typically, a buffer tank is smaller than a storage tank. Anyway, in this work, the tank volume is not fixed; for instance, in the study presented in Chapter 5, it is considered as a parametric value. In some other cases, the DHW tank is modelled with the non-standard type 340 using 5 nodes, with a temperature sensor for control in node 2.

2.2.2 Building and emission system

As mentioned in the introduction, the HVAC system under analysis is deeply connected with the building that it is serving. Consequently, its performance is expected to be dependent on the building dynamic behaviour. In the following, the majority of the studies involve a single-family house, which was modelled using type 56 of the standard TRNSYS library.
In this model, the heat fluxes that characterize the thermal behaviour of any wall or window include: the conduction heat flux (from the inside to the outside surface or vice-versa), the convective heat exchange with the air, and the radiative heat exchanges with all other surfaces. Shifting the focus to the airnode balance, the convective heat gain is defined as the sum of the convective gain from surfaces, the internal convective gains (by people, equipment, illumination, radiators, etc.), the fraction of solar radiation entering an airnode through external windows (which is immediately transferred as a convective gain to the internal air), the absorbed solar radiation on all internal shading devices of zone (directly transferred as a convective

gain to the internal air), the gains due to air flow from other airnodes or boundary condition, and the infiltration gains (air flow from outside only). The radiative gain for the wall surface is defined as the sum of the radiative airnode internal gains received by wall, the solar gains through zone windows received by walls, the long long-wave radiation exchange between this wall and all other walls and windows, and the user-specified heat flow to the wall or window surface. The geometry of the building that is taken as reference in the majority of the following analyses is a two-floor single-family house and it is shown in Figure 2.1. It has a volume of 275 m^3, façades oriented towards the main cardinal directions and window exposure toward south, east, and west. The choice of this building is due to a previous modelling work of a real experimental building, for which thermal variables have been monitored for several years. However, this thesis does not concern any experimental study. The envelope characteristics were changed so as to adapt the model to the particular simulation work. The geometry and the floor area (about 80 m^2), are maintained constant in the different simulation scenarios. The dimension can be considered representative of a European family house, since the European average floor area of the residential dwelling is 84 m^2, according to statistics (ENTRA NZE, (Enerdata, 2008)). The building model is divided into four thermal zones, three of which are equipped with heating and cooling terminals. The utility room has not heating/cooling terminal but only the internal gain due to the tank thermal losses. South-facing windows have a shading factor of 0.5 during the cooling season only. No other shading elements were considered, neither for the opaque part nor for the glazed part of the envelope.
In other studies (see Table 2.1) a simpler building with a single thermal zones is modelled (Figure 2.2). This is considered a semi-detached house, as an adiabatic boundary condition is imposed to one wall, whereas all the

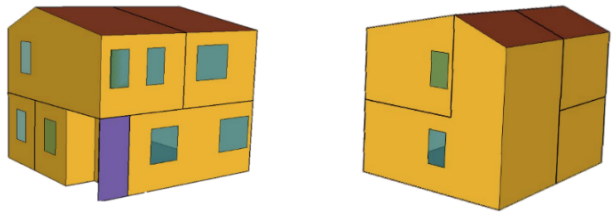

Figure 2.1: *Two floors house model with four thermal zones.*

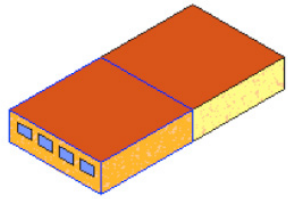

Figure 2.2: *Simple semi-detached house model with one thermal zone.*

other surfaces are directly exposed to the external environment. This building, which geometry and characteristics were previously defined in (Penna et al., 2015), has 100 m^2 floor, façades oriented towards the main cardinal directions and a south window exposure.

Both the building models have an integrated radiant floor model ("active layer", included in the TNRSYS type 56). The layer is called "active" because it contains fluid filled pipes that either add or remove heat from the surface. The modelled radiant floor design is based on a typical commercial configuration with cross-linked polyethylene pipes having a diameter of 0.016 m, a thermal conductivity of 0.44 $Wm^{-1}K^{-1}$, and spacing of 0.12 m,

immersed in a concrete screed with a thickness of 6 cm. The radiant floor is used for SH only, whereas cooling (when present) is achieved by means of fancoils, which are simulated with type 508. Type 508 can operate either by controlling the outlet air dry bulb temperature/humidity or in the unrestrained (uncontrolled) mode, in which the coil cools and dehumidifies the air stream as much as possible given the inlet conditions of both the air and the fluid streams. The latter operation mode is assumed throughout this work.

In other studies discussed in this thesis, in particular those referring to a Swedish scenario, the simulated building is a typical Swedish detached single-family house, characterised by a single floor, an overall U-value of 0.2 W $m^{-2}K^{-1}$, and 143 m^2 of floor area with a radiant heating system. The design of this house is obtained from the catalogue of the Swedish leading company of detached houses and it is almost always built with an exhaust-air heat pump. A detailed model of the house with six zones is developed in the simulation software TRNSYS and it was validated by (Persson and Heier, 2010). Hereafter, the basic characteristics are discussed. Different electrical appliance gains and occupational profiles are applied to the proper zones in the building, whereas, in the zone representing the utility room, heat losses from the compact HP system (including DHW store) are applied as internal gains. The two bedrooms and the utility room have a set temperature equal to 20°C, the bathroom 22°C, and the other two zones (living room and kitchen) are set at 21°C. The model also accounts for the heat transfer between zones due to doors opening, which is rarely modelled. This model is also used by (Leppin, 2017), in which an additional detailed description of the building can be found.

2.2.3 Other system components

The overall system is completed by several other components, on which an overview is provided in the following:

- a PV array is modelled with type 194, which, based on the calculation method presented by DeSoto (De Soto et al., 2006), determines the electrical performance of a PV array using a five parameter model;

- a lithium ions battery fractional state of charge (FSOC) is defined by means of the following equation; a charge/discharge rate of 1C, deep of discharge 80%, and efficiency 95% are assumed.

$$FSOC = \begin{cases} \int P_{battery}(t)\mathrm{d}t, & P_{battery}(t) \leq P_{battery,max}, \\ \int P_{battery,max}\mathrm{d}t & P_{battery}(t) > P_{battery,max} \end{cases} \tag{2.6}$$

  where $P_{battery}(t)$ is the power exchange with the battery (positive when power flows towards the battery and negative for the opposite direction) and $P_{battery_max}$ is the charge (positive) or discharge (negative) power rate (numerically equal to the battery capacitance). The minimum and maximum values of $FSOC$ are 0.2 and 1, respectively;

- a heat recovery ventilation system based on TRNSYS type 760 is used to transfer sensible energy from the exhaust air exiting the building to the fresh air entering the building (or vice versa in the summer), assuming a recovery efficiency of 75% and an electric consumption of the fan of 3 $\mathrm{kWm^{-3}s}$;

- minor components, such as the pumps (type 110), the diverter and mixer valves (standard type 11 and TESS types 647/649), or the pipes (type 31) are not described in details. Component belonging to

Table 2.1: *Layout of simulations performed in the various papers. Paper 2 is not based on dynamic simulation*

	DHW	**PV**	**Battery**	**Climate**	**Building thermal zones**	**HP model**	**time step** [*min*]
Paper 1	×	×	×	Northern Italy	1	air-source TC model	5
Paper 3	×	✓	✓	4 EU cities	1	air-source TC model	5
Paper 4	✓	✓	✓	Norrköping (Sweden)	6	exh. air-source perf. map	1
Paper 5	×	✓	✓	3 IT cities	1	air-source TC model	5
Paper 6	✓	✓	×	Northern Italy	4	air-source FC model	1
Paper 7	✓	×	×	Northern Italy	4	air-source FC model	1
Paper 8	✓	✓	(✓)	9 EU climates	4	air-source TC model	1
Paper 9	✓	✓	(✓)	Norrköping (Sweden)	6	exh. air-source Type 581	1
Paper 10	✓	✓	×	Northern Italy	4	air-source FC model	1

the control system, such as thermostats, forcing functions, and other equation and algorithms are described in Chapter 5.

While all of these components are considered, not necessarily all of them are simultaneously active in each simulation scenario of this thesis. The system layout is reported in Figure 2.3. Table 2.1 details the system composition for each of the studies reported in this thesis involving dynamic simulation.

2.2.4 Boundary conditions

This section provides the sources or the definition method for the boundary conditions, *i.e.*, those variables which are input with respect to the

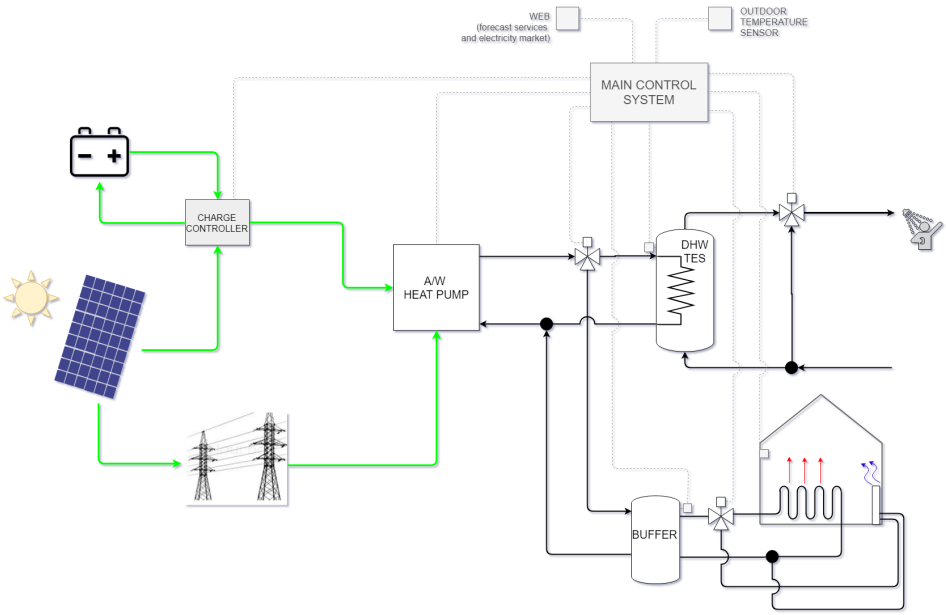

Figure 2.3: *Complete system layout.*

simulated system and are a function of the time.

Weather As pointed out in (Arteconi, 2018) and (Tian et al., 2018), weather data is one of the main sources of uncertainty in building simulation. However, depending on the purpose of the simulation, different uncertainty levels can be accepted. A typical choice is using a representative year obtained from historical data, and this is considered an acceptable approximation for the purpose of this thesis. Multiple years simulations would improve the estimation of the building system KPIs. For instance, actual measures of the last 10 years would be more representative of the recent climate changes. Of course that would increase the computational time. The me-

teorological variable of interest as boundary condition for the system are: global horizontal radiation, dry-bulb temperature, relative humidity, and wind speed. The weather data file used are the IWEC data files (International Weather for Energy Calculations, n.d., Atlanta), which are "typical" year data. "Typical" weather files are more suitable for use with building energy simulation programs than test reference year (TRY) type weather data, which are single-year data, since the latter cannot represent the typical long-term weather patterns, (Crawley, 1998). Many locations in Europe have been referred to in the various studies. An overview is provided in Table 2.1. When referring to Northern Italy, the considered reference location is Milan, which has a 4A climate according to ASHRAE classification (2001). The typical meteorological years (TMY) provided by CTI (CTI, 2015) were used. The data were obtained by CTI in collaboration with ENEA (ENEA, 2011, 2012) according to the procedure described in the UNI EN ISO 15927-4 standard and consist of 12 characteristic months chosen from an archive of meteorological data recorded for a time period preferably greater than 10 years. The months have been chosen from different years of the period for which the climatic data are arranged and then merged to form the year (correcting the transition points between one month and another). The typical climatic years represent, in the long term, the average values of the most important climatic parameters (temperature, relative humidity, global irradiance on the horizontal plane, and wind speed) and are characterized by realistic dynamics and a real correlation between different climatic parameters, in particular between temperature and global solar irradiance. However, it is worth noticing that CTI refers to those time series with the acronym TRY, whereas the series reconstructed by means of that procedure are more commonly referred to as TMY.
A different approach is used in Paper 4 and Paper 9. Meteorological data

for the location of Norrköping (Sweden) are used. Measured high-resolution (one minute) time series from the year 2015 are provided by the Swedish Meteorological and Hydrological Institute (SMHI).

DHW tapping profiles The DHW load profile is obtained from the tapping programs in EN 15316-3-1:2008 (subsequently replaced with EN 12831-3:2017 (European Commission, 2017)) for single family dwellings (average daily tapping pattern for a family with shower use). In particular, tapping program No. 2, which is representative of an average European use, is selected and implemented in the simulation. Since the profiles are provided in terms of time of the day at which the tapping starts and the relative energy in [kWh], the data are elaborated in order to obtain hot water flow rate values at constant time intervals by assuming a temperature difference of 30K and maintaining the energy. in Paper 4 and Paper 9 (*i.e.*, one minute), a more detailed DHW tapping profile is required. The model of the DHW demand complies with (Bales et al., 2015). It was originally derived with the program DHWCalc developed by Jordan (Jordan and Vajen, 2005).

Occupancy People presence is modelled by means of a static schedule with a weekly pattern, which represents the total internal gain given by the people and the appliances. Despite its poor reliability, (Dong et al., 2018), the static schedule is the most popular occupancy modelling technique, especially in studies that are not focused on the occupants' behaviour. Two different profiles for the living room/ kitchen and for the bedroom are provided in the Italian standard UNI-TS 11300 (UNI, 2016*b*,*a*) and are shown in Figure 2.4. In TRNSYS, it is implemented with type 14. Only in one of the analyses here presented a stochastic occupancy model is used.
In Paper 4 and Paper 9, the occupancy model is more detailed; in particular,

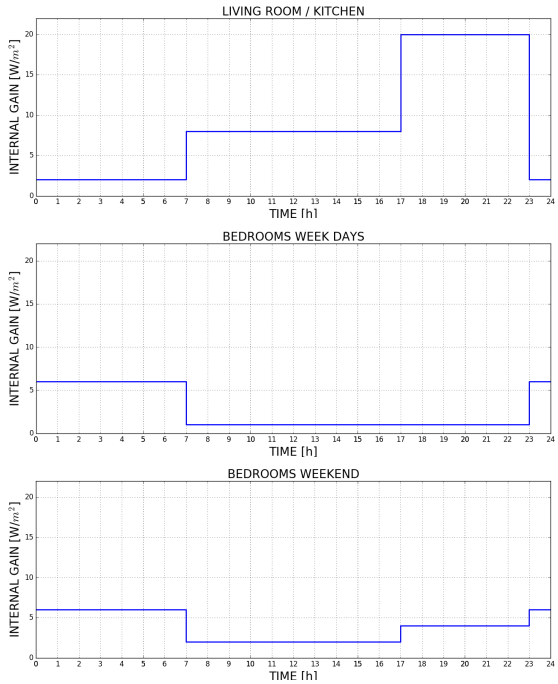

Figure 2.4: *Internal gains profiles due to occupancy and appliances. The profile is provided in the Italian technical specification UNI TS 11300-1(UNI, 2016*a*).*

two adults and two children are assumed to be living in the house and the internal energy gain due to their presence, and their use of appliances, is computed using a Markov-chain model for occupancy and energy use (including lighting) as described in (Widén and Wäckelgård, 2010). The occupancy profiles cover a complete year and have a one minute resolution.

Electricity price Within this thesis, some studies involve electricity tariffs. In particular, they refer to either an Italian or a Swedish context.

Swedish scenario. For Sweden, both the variable monthly tariff (flexible tariff scenario) and dynamic hourly spot market price from Nord Pool (Swedish Energy Agency, 2018) are considered. The dynamic energy price is a relatively small fraction, approximately one third, of the total end-user price. The purchased electricity price also includes the grid fee, the electricity certificate, and the value added tax. For the feed-in electricity to the grid, only the spot market price and the electricity certificate are considered. This is likely to become the mainstream scenario in the near future when subsidies are reduced. In the case of hourly spot market price, the utility fees for the end user are accounted as 0.07 €cent/kWh for purchased electricity and 0.015 €cent/kWh for electricity fed to the grid (from 2015 market data, (Swedish Energy Agency, 2018)). The typical daily profile of the real time pricing presents a double peak (one in the morning and one in the evening) due to the combination of the average demand and the renewable (PV) input to the grid. The peaks may become more relevant in case the PV share of the total electricity production increases. For this reason, in one of the studies, an hypothetical price profile is introduced, in which the deviation from the daily running average is doubled. Figure 2.5 shows an example of the amplified electricity price profile, in the first week in January 2015.

Italian scenario. In simulations involving the Italian electricity prices, both the domestic user tariff, having two price levels along the day, and the small-commercial Italian tariff for the year 2017 are considered. The latter, which is expected to be applied also to domestic users in the near future, has three price levels along the day (applied on the base of the time of use), and it is updated on a monthly base. The variable part of the total cost includes transport/management and system charges. In addition, the hourly spot market price (real-time pricing) is applied and its time evolu-

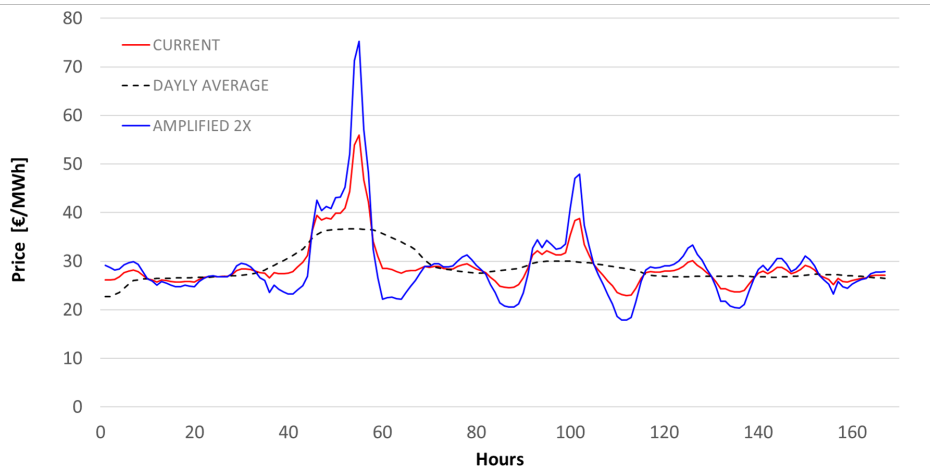

Figure 2.5: *Amplified electricity price deviation from the 24h running average (example of the first week in January 2015).*

tion is supposed to be known in advance. It is less likely that the real-time pricing will be applied to domestic users in the near future in Italy (as it is in other countries), but it still may be one of the possible scenarios. Both in the case of time-of-use (TOU) tariff and real-time-pricing (RTP), the total electricity bill also includes a fixed annual tariff and an average share of 13% of fees. Figure 2.6 shows the real-time prices (day-ahead market) for the winter season in 2017, net of fixed annual costs and taxes.

2.3 Key Performance Indicators

In the following, a list of the various KPIs that are referred to in the next chapters is presented.

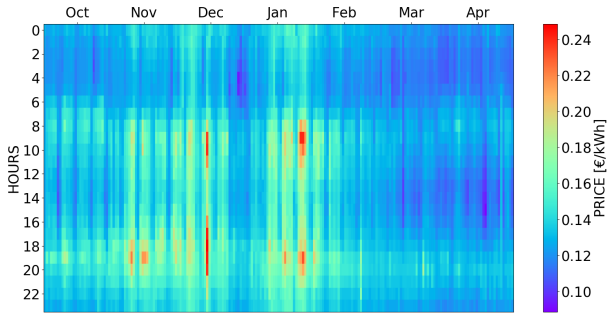

Figure 2.6: *Italian real-time hourly pricing (below) for year 2017. Prices include transport/management and system charges but annual fixed costs and taxes are not included.*

Heating and cooling demand The heating demand mainly depends on the building envelope and on the climate of the region in which the building is located. However, it is also influenced by other variables, such as the occupants' presence and behaviour, the ambient set-point temperature, and the ventilation rate. The heating and/or cooling thermal energy demand can be expressed in terms of total annual energy or divided by the floor area (kWhm^{-2}). Finally, it is worth noticing that it is different from the heating and cooling consumption, which typically refers to the whole system, including the HVAC system (*i.e.*, the final electric energy use, which can include the PV contribution or not).

Final energy The annual final energy use for the simulation period (FE) is equal to the electric load that cannot be supplied by PV electricity and must be purchased from the grid. In some analyses, this quantity is also referred to as energy from the grid ($E_{fromgrid}$).

PV self-consumption The energy directly taken from the PV or from the battery is here referred as self-consumption (SC). SC is the integral over time of the corresponding power, P_{SC}, evaluated in a generic observation period T_{obs} (*e.g.*, one month or the season) as shown in eq. (2.7) . Therefore, in a system connected to the grid, the sum of the self-consumption SC and the energy delivered to the grid (GI, grid input or E_{togrid}) corresponds to the net PV production over the considered observation period. The SC can also be expressed as fraction, SC_r, of the net PV production, as in eq. (2.8):

$$SC = \int_{T_{obs}} P_{SC}(t)\mathrm{d}t \tag{2.7}$$

$$SC_r = \frac{SC}{\int_{T_{obs}} P_{PV}(t)\mathrm{d}t} \tag{2.8}$$

Solar fraction Since in this work the solar energy is exploited only by means of the PV (no solar thermal collectors), the solar fraction of the consumption is defined as the self-consumption from PV divided by the total energy use:

$$SF = \frac{SC}{\int_{T_{obs}} L(t)\mathrm{d}t} \tag{2.9}$$

Aerothermal share The aerothermal (renewable) energy can be calculated in periods when the HP is working in heating mode (Shibata, 2011). The classic scheme of a HP energy balance reported in Figure 2.7 is meant to identify the aerothermal contribution, which is computed as the difference between the usable thermal energy (for heating or DHW) and the electric energy use.

Renewable share The aerothermal and solar energy contributions can be summed to obtain the renewable energy use, which is also an important

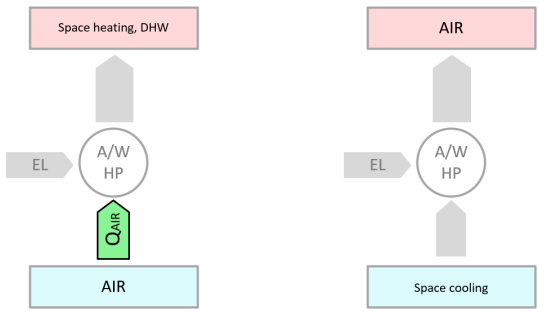

Figure 2.7: *The arothermal (renewable) energy use in the HP operation is highlighted.*

KPI in some analyses. More precisely, the global renewable share should also include the electric energy use of the HP multiplied by the share of the electricity production from renewable sources in a specific country. However, it is often preferable not taking into account this contribution, so that the KPI is referred to the system only.

Primary energy use The primary energy is a key indicator often used to compare different types of thermal energy generation to each other. In the case of a electric-driven system, such as the HP system, the primary energy is calculated by multiplying the electricity use by the primary energy factor (PEF) of the country of interest. The European PEF value is 2.5, which means that each unit of electricity requires an input of 2.5 units of primary energy. However, as reported in (Esser and Sensfuss, 2016), the PEF would need to be revised (lowered) since the current one is based on old data reflecting a European power system without any significant share of renewables in the power generation mix.

Seasonal coefficient of performance and energy efficiency ratio The COP and the energy efficiency ratio (EER) of HPs are typically evaluated with the heat pump operating at steady-state conditions. However, over a long period (*e.g.,* the season), the average performance of the machine can be significantly different. The respective seasonal performance rates (SCOP and SEER) are defined in eq. (2.10). Despite the SCOP can also be referred to the whole generation system, including the back-up heating [1], if not otherwise indicated throughout this work this value is referred to the machine, which means that the denominator only includes the electric energy absorbed by the compressor and other minor devices embedded in the unit. In (2.10), providing the SCOP, T_{obs} is the generic observation time; the SEER is calculated in the same way, in a observation time during which the HP is operating in the cooling mode.

$$SCOP = \frac{\int_{T_{obs}} P_{HP,th}(t)\mathrm{d}t}{\int_{T_{obs}} P_{HP,el}(t)\mathrm{d}t} \tag{2.10}$$

Seasonal performance factor Unlike the above mentioned performance indicators (SCOP and SEER) that refer to the HP performance, the seasonal performance factor (SPF) refers to the system performance over a time period (typically over the heating or cooling season). The SPF is here defined as the ratio between the final thermal energy use (for SH, cooling, and/or DHW) and the total electric energy absorbed by the system, including the various electric devices in the system (*i.e.*, in this thesis, fans, fancoils, pumps). This indicator implicitly takes into account of the system

[1] Different values of SCOP are proposed in the European standard EN 14825 (European Commission, 2016), where the $SCOP_{on}$ includes the electric back-up heater. The standard applies the bin method to calculate the seasonal performance

losses and it is therefore typically lower than the SCOP/SEER, unless free thermal energy gains are considered.

Annual cost The operating cost is considered in some of the studies of this thesis. However, the initial investment cost of the system is not considered. The operating cost for electric-based system is the cost of the electricity, which typically includes shares for energy supply, delivery, management and taxes. In some cases, as the householder receive a revenue for the energy delivered to the grid, the annual net cost of electricity (NCOE), also referred to as "net bill" is defined as the difference between the total cost (or bill) and the revenue.

Net present value The NPV is calculated as an objective function to be minimized in Paper 5 and it quantifies the economic benefits of a design solution. The analysis is based on a lifespan that was considered equal to 30 years. The NPV takes into account the initial investment cost, the annual running costs, the maintenance cost, the replacement costs, and the residual value, according to the standard EN 15459 (European Commission, 2007). The initial costs were defined starting from a market survey, by defining a pattern of costs as a function of the main product characteristics. In particular, the initial costs (IC in [€]) for an air-source HP (IC_{ASHP}), a water storage tank (IC_{stor}), a PV array (IC_{PV}), and an acid-lead battery (IC_{batt}) were defined. The following equations are derived from a market survey, by defining a pattern of costs as a function of the main product

characteristics:

$$IC_{ASHP} = COP_{rated}^{2.1305} \left(127.03 + 20.71 \cdot \phi_{rated}\right) \quad (2.11)$$

$$IC_{stor} = 2.60 \cdot 10^{-3} \cdot V_{stor} + 456.4 \quad (2.12)$$

$$IC_{PV} = 1550 + 862.5 \cdot n_{str} \quad (2.13)$$

$$IC_{batt} = 0.274 \cdot Q_{batt}^{0.9376} \cdot n_{batt} \quad (2.14)$$

where ϕ_{rated} is the rated ASHP thermal output at 7/35°C [kW], V_{stor} the volume of the storage tank in [liter], Q_{batt} the capacity of a single lead-acid battery in [kWh], and COP_{rated} the full load rated COP at 7/35°C.

CHAPTER 3

Performance evaluation and system sizing

3.1 Evaluation of the performance at part load operation

The approach of HVAC designers to the HP sizing can be difficult due to the limited knowledge of the machine behaviour, especially at part load operation. However, the impact of considering the part load operation in the sizing procedure of HP systems and in assessing their seasonal performance has long been recognized. When these machines are dimensioned for design conditions (*i.e.*, for the lowest air temperature in case of heating operation), they work at part load for most of the season. For a correct evaluation of this behaviour, it is necessary to consider the real load profile of the building and the climate of the geographical zone, as well as to know how a particu-

lar machine works with variable conditions. Furthermore, the optimal size depends on whether it is a fixed or modulating heat pump (Dongellini et al., 2015). Notably, the most accurate performance evaluation - excluding the field measurement, which is not possible in case of design evaluations - is the dynamic simulation. If the thermal inertia in the dynamic simulation is neglected, the difference of performance in terms of $SCOP_{net}$ (as defined by UNI EN 14825) between the dynamic method and the bin method is rather limited (Naldi et al., 2015). However, the thermal inertia impact may be significant in systems with thermal storage tanks and high thermal capacity buildings. The dynamic method is applied in all the studies reported in this thesis, except in Paper 1, in which the bin method is applied; in Paper 2, a comparison between the bin method and the dynamic method is discussed. In any case, the dynamic approach is not widespread today among system designers. In terms of standard regulations, calculation procedures have been developed seeking a compromise between the complexity of the methodology and the accuracy of the results (Baggio, 2013). To compute the heating needs with heat pumps, the standard UNI TS 11300-4 (UNI, 2016*b*) suggests the monthly bins method, based on the reconstruction of the hourly temperature distributions from average monthly climate data. For the province of Trento, those temperature distributions are shown in Figure 3.1a. A similar procedure is described in the standard EN 15316-4-2 (European Commission, 2008). However, this method is rather complex and not very intuitive: the bin method can be applied more directly starting from the typical meteorological year, which is available for all Italian provinces, as shown in Figure 3.1b for the province of Trento.

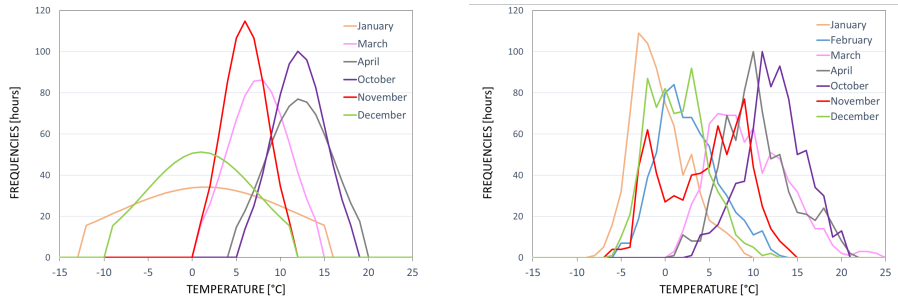

(a) (b)

Figure 3.1: *Monthly curves of the external temperature distribution for the province of Trento, obtained with the method of the UNI TS 11300 - 4 (a) and from the typical year (b).*

3.2 Impact of temperature distributions modelling

As assessed in Paper 1, applying the bin method to the distribution curves according to the procedure of the Italian legislation cited above or to the typical year data, leads to different results. In the study, a hypothetical building with a floor area of 120 m^2 was adapted in order to obtain annual heating demands of 60 $kWhm^{-2}$ (B60) and 120 $kWhm^{-2}$ (B120). The monthly energy signature (*i.e*, the required heating power as a function of the external temperature) is reported for the case of the building B60 located in the province of Trento, Italy, as shown in Figure 3.2. The curves on the left are obtained by means of the method suggested in the Italian standard UNI TS 11300 - 4 and those on the right by using the frequencies distribution obtained from the typical year. In both cases, the months of April and October show a lower required power (with respect to winter months), with the same external temperature, due to the greater solar gain. At 20 °C, the load is zero by definition.

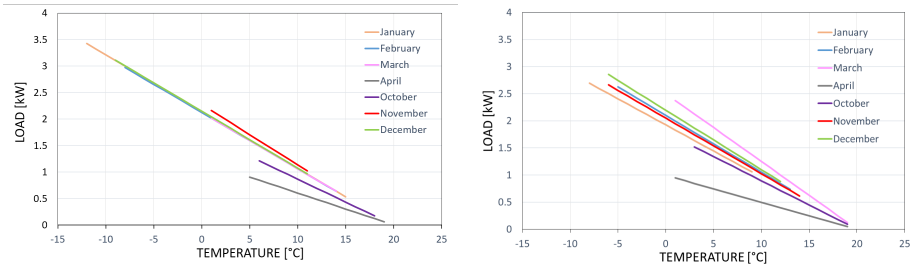

Figure 3.2: *Monthly curves of the heating need of the building B60 located in Trento, calculated from the temperature distributions obtained with the method of the UNI TS 11300 - 4 (left) and from the typical year (right).*

The procedure described above was applied to the climate of all the Italian provinces. The building load does not vary with the location. The calculation is made for 2 different loads, corresponding to the heating needs of 60 $kWhm^{-2}$ and 120 $kWhm^{-2}$. Results are presented in the form of a national map (Figures from 3.3 to 3.6). The main objective of the analysis is the comparison between the two discussed methods; therefore, all results are represented in terms of variations. First, it can be observed that, in general, there is no systematic overestimate in using one method over the other. The difference depends on the considered province. For some provinces, the application of the UNI TS 11300 method gives higher SCOPs and loads coverage values, while, for others, a more favourable situation is estimated by using the typical year data. The higher differences between the two methods occur in some provinces of Sicily, Calabria, and Campania, for which the typical year gives higher shares of electric energy attributable to the heat pump with respect to the total electric consumption, which includes the share of the auxiliary heater.
Still referring to this index, for some provinces of the Apennines (Lucca,

Arezzo, Rieti, L'Aquila, Benevento, Avellino), in addition to Aosta, Taranto, and Brindisi, the application of the UNI TS 11300 method provides more favourable values. Another interesting observation is that the evaluation of the SCOP is more sensitive to the applied method in the case of modulating HP. The SCOP deviations between the two methods are between -0.30 and $+0.20$ for inverter heat pumps and between -0.13 and $+0.11$ for on/off heat pumps. For modulating heat pumps, the relationship between the load curves (Figure 3.2) and the external temperature distribution is more relevant, since this determines the load factor CR for each bin. On the one hand, the differences in terms of seasonal performance are very limited. On the other hand, considerable differences are found in the evaluation of the auxiliary energy share. This information is contained in the e_{pdc} index (Figures 3.6 and 3.5), defined as follows:

$$e_{pdc} = \frac{E_{el,pdc}}{E_{el,pdc} + E_{el,aus}} \tag{3.1}$$

where $E_{el,pdc}$ is the amount of energy related to the heat pump and $E_{el,aus}$ is the one related to the auxiliary electric heater. It can be noticed that for the building with greater demand (of which the pdc does not cover peaks), there are differences greater than 30% between the two methods, in terms of e_{pdc}; the differences are instead limited for the building with a requirement of 60 kWhm^{-2}.

To summarize, this study shows that the bin method gives different results depending on whether it is applied to the distribution curves built according to the Italian normative procedure (UNI TS 11300-4, Appendix G) or to the typical year data series. However, the differences cannot be generalized for the Italian territory (it depends on the particular zone). The deviations in terms of net seasonal performance of the heat pump are greater in the case of a modulating heat pump (maximum SCOP differences of 0.3). Greater

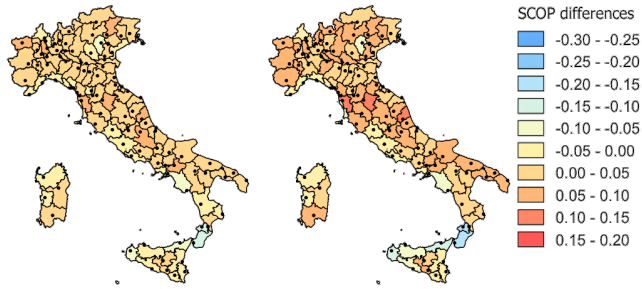

Figure 3.3: *SCOP for the on/off HP; variation of the values obtained with the UNI TS 11300-4 bin method with respect to the bin method applied to the typical year. Building with* 60 $kWhm^{-2}$ *(left) and* 120 $kWhm^{-2}$ *(right).*

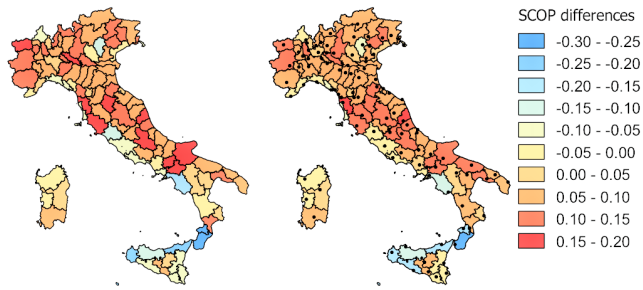

Figure 3.4: *SCOP for the inverter HP; variation of the values obtained with the UNI TS 11300-4 bin method with respect to the bin method applied to the typical year. Building with* 60 $kWhm^{-2}$ *(left) and* 120 $kWhm^{-2}$ *(right).*

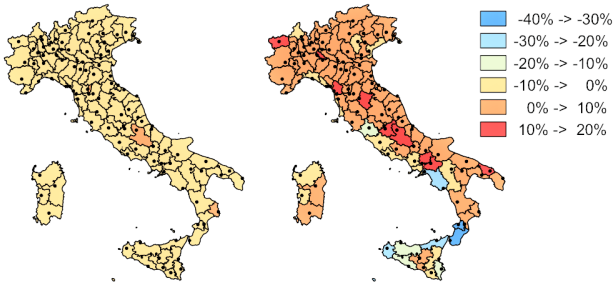

Figure 3.5: *Share of electrical consumption of the on/off HP, in the hypothesis of electrical back-up; percentage variation of the UNI TS 11300-4 bin method with respect to the bin method applied to the typical year. Building with* 60 $kWhm^{-2}$ *(left) and* 120 $kWhm^{-2}$ *(right).*

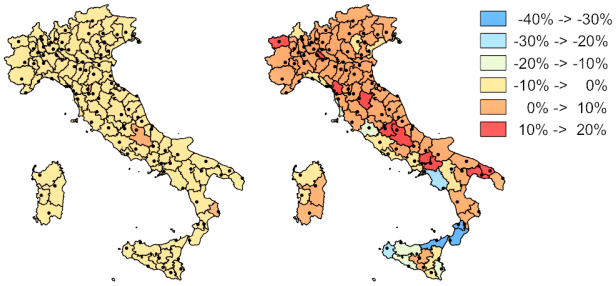

Figure 3.6: *Share of electrical consumption of the inverter HP, in the hypothesis of electrical back-up; percentage variation of the UNI TS 11300-4 bin method with respect to the bin method applied to the typical year. Building with* 60 $kWhm^{-2}$ *(left) and* 120 $kWhm^{-2}$ *(right).*

differences are shown in terms of share of the heating demand covered with the HP and, consequently, of auxiliary energy to satisfy the totality of the load, a quantity that should be assessed with accuracy in order to correctly design residential heating systems. Both methods are affected by uncertainty, which has not been evaluated and which is difficult to avoid with stationary calculation methods. However, the method suggested in the legislation involves a greater complexity of application which is hard to justify, given the availability of hourly climate data (*i.e.*, the possibility to apply the method of monthly bins directly to these data). Furthermore, with hourly data it is possible to take into account, for instance, the different use of the system between day and night, thus distinguishing between day and night bins, or depending on different user profiles (*e.g.*, offices). Finally, the typical years also provide humidity data, an information that the designer might use for more realistic assessments of the actual performance of a particular installation. These investigations are clearly impossible with the method proposed by the legislation.

3.3 Impact of part load performance modelling

In Paper 2, the TC model described in Chapter 2 is used for the dynamic simulation of the heat pump operation at part load conditions. In this study, the impact of the COP variation (*i.e.*, the choice of the correction function) on the seasonal performance was analysed. Two different calculation procedures were compared to each other: the bin method and the dynamic method. The simulation scenario is typical of the mountain area in Northern Italy (climatic data for Trento, Italy) and the building is the one described in Section 2.2.2. With the reference design temperature of $-12°C$, the design load calculated according to EN 12831 (European Com-

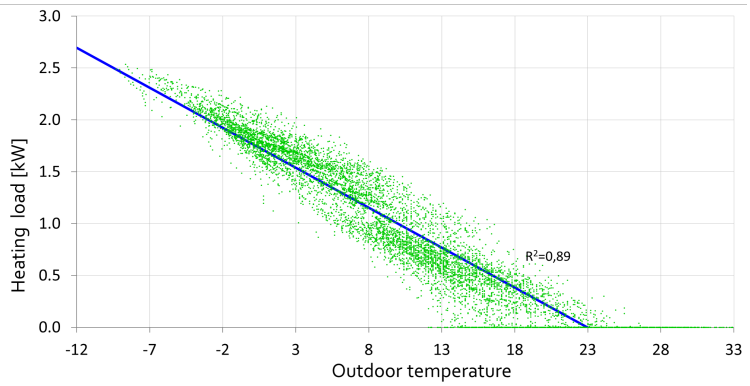

Figure 3.7: *Heating power required by the building as a function of the external air temperature. The blue line is the linear regression (i.e., Building Energy Signature).*

mission, 2017) is 4.1 kW. Figure 3.7 represents the heating power required by the building as a function of the external air temperature. The green dots correspond to the average hourly values resulting from the dynamic simulation of the building (simulated without the heating system). The linear interpolation is extended to the project temperature ($-12°$C according to EN 12831) and the corresponding heating power is 2.7 kW. This value is only 66% with respect to the calculated one. This can be justified by considering that the temperature of $-12°$C is not reached in the typical year time series (which is used as input in the simulation) and that the calculation procedure in the EN 12831 does not consider solar gains (the design power is calculated in order to preventively taking into account the worst possible condition). In order to highlight the differences in the results obtained by using the bin method and the dynamic simulation, a simplified configuration is used in the dynamic model: the thermal capacity is neglected (*e.g.*, no storage tank and/or envelope mass is considered), and

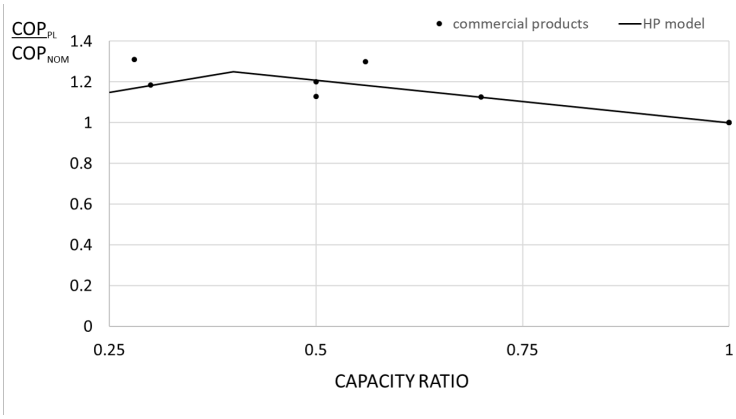

Figure 3.8: *COP at part load operation. The points show the performance variation of some commercial products with respect to the nominal one and the line is the parametric curve that can be changed in the HP model.*

the building load has been assumed to vary according to the energy signature curve of the building (shown in blue in Figure 3.7). Looking at Figure 3.8, the ratio between COP_{PL} (COP at part load) and COP_{NOM} (COP at nominal condition), which also corresponds to the correction factor f_{corr} introduced in Section 2, is not constant for varying capacity ratios (CR). The dots refer to some products (different brands) in the market and the line represents a parametric curve which is implemented in the HP model (Section 2.1). The parameters that define this curve are the maximum f_{corr} and the corresponding CR at which the maximum occurs.
Overall, the performance is evaluated in three cases:

- a function obtained from the above mentioned parametric curve, with a maximum $f_{corr} = 1.2$ at $CR = 0.55$, which is intended to represent one of the products available in the market;

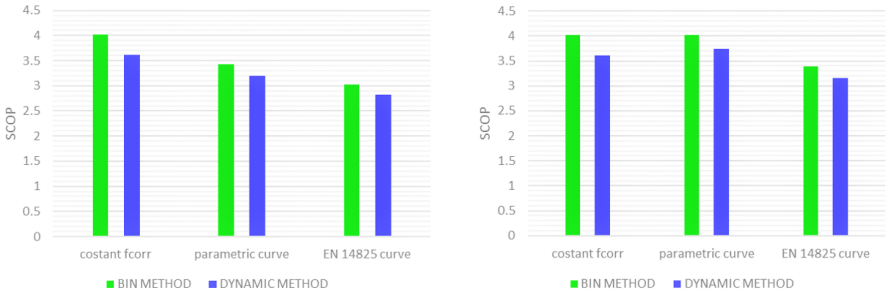

Figure 3.9: *Seasonal performance of two different HP sizes (i. e., thermal power): 80% of design load (left) and 60% of the design load (right). Calculation with bin method (green) and dynamic method (blue).*

- a constant f_{corr} (equal to 1), for any CR value (*i.e.*, the COP variation is not considered at all);
- a COP degradation function as proposed by the standard EN 14825, already described in section 2.1.

For each case, the SCOP is evaluated, by using both the bin method and the dynamic simulation method. Two different HP nominal capacities (corresponding to 80% and 60% of the design load of 4.1 kW) are considered. The results are shown in Figure 3.9. The histogram clearly shows that, when the performance variation is not taken into account, it is not possible to appreciate the performance difference between two sizes and the performance is overestimated with respect to the other cases, in which the performance variation at part load is considered. On the contrary, by applying the f_{corr} suggested in the standard, a poorer seasonal performance is obtained. Although the difference between the SCOP obtained with the two methods is rather limited, the dynamic method gives lower SCOP for all of the considered cases. After performing the dynamic simulation with the simplified

method, other elements were introduced in the dynamic model, such as the building complete model (in place of its energy signature curve) and a buffer tank. In this case the SCOP slightly increases. To summarize, the bin method can give numerical results in good agreement with dynamic hourly simulation, as long as the dynamic model does not consider the benefits arising from inertial elements, such as thermal water storage systems and a massive envelope and from a climatic control of the system. When such effects are considered, the overall performance is improved: this condition can only be simulated with a dynamic model.

3.4 Impact of the system sizing

The size of the main components of the system (heat pump, water tank, PV) strongly influences the behaviour and the performance of the system itself. However it is not trivial to determine the optimal size of a component, since it depends on the objective and on the scenario. (Beck et al., 2017) analysed the influence of various scenarios on the optimal dimensioning of cost-effective self-consumption driven heat pump systems. In the following, some observations are made on the heat pump and the water tank sizing.

3.4.1 Heat pump sizing

Typically, a heat pump is not sized to completely cover the heating demand of a building. According to (Fischer et al., 2016), who analysed different manufacturers guidelines and textbooks, the HP unit is sized to cover approximately 95% of the total annual heat demand. During thermal peak hours, an electric back-up heater supports the HP; however, this is not sufficient to decide the HP optimal capacity. The simulation is useful to understand the behaviour of the system and it allows us to try different

combinations of HP size and back-up heater activation periods. Going back to Figure 3.9, the small HP seems to perform better, as its size is closer (91%) to the design load calculated by means of a dynamic simulation (which is sensibly lower than the one calculated according to the standard). The larger size operates for a longer time under the modulation limit, and therefore with on/off operation, which degrades the seasonal performance. The appropriate sizing of the HP is still a key issue in order to achieve the most efficient operating conditions not only for the on/off units, but also for inverter driven HPs. The best approach seems to be to under-size the HP capacity with respect to the design load, carefully optimizing the best combination of an HP and an auxiliary heating source (that presumably will operate for a limited time) by means of dynamic simulation. Finally, an additional conclusion from the results of Paper 2, is that a lower HP size, such as $60 - 70\%$ of the (effective) design load, does not necessarily require to largely use the electric heater. An under-sized HP will operate at full load for most of the time and it will be able to cover a significant share of the load (*i.e.*, the reduction of this share is not as large as the reduction of the size).

3.4.2 Thermal storage sizing

Another key aspect of the system is the storage capacity. In particular, it is important to correctly size and control the system storage elements, in order to maximize the renewable coverage share and overcome the shift in time between PV production and energy demand. As assessed in (Arteconi and Polonara, 2018), thermal energy storage can provide flexibility to the system, by means of load shifting. If properly controlled, thermal storage capacity can also reduce the energy bill, although it generally increases

the energy use because of thermal losses, (Arteconi and Polonara, 2018; Arteconi et al., 2013). Paper 5 addresses the sizing aspect by analysing the mix of total storage capacity between thermal storage tank, lead acid battery, and thermal capacity of the building envelopes for an optimal design solutions in three Italian climates. Figure 3.10 shows the Pareto front solutions for the three climates, as a function of the water storage volume, and Figure 3.11 shows the cumulative distribution function (CDF) of the tank volume values belonging to the Pareto solutions. The 60% of the solutions in the Pareto front has a volume lower than 150 liters in Trento and Rome, whereas in Palermo the 0.6 fractile is equal to 100 liters. The transition from the 0.6 fractile to the 0.99 fractile implies an increasing of the tank volume of about two times in Trento and Rome and three times in Palermo. More in general, it can be observed that in almost all of the optimal solutions, the volume of the storage tank is rather low with respect to the considered range (the same applies to the battery capacitance) and this would suggest that energy storage is not economically convenient in this system. However, it is worth noticing that, in this simulation, the system control is not designed for any particular demand-side management strategy. But yet, this ‘ ‘default” control is more representative of the actual installations of those systems nowadays.

Also in Paper 3 the thermal storage aspect is addressed. The main finding is that increasing the tank size in the range of the typical installations has only a slight effect on the self-consumption percentage. The impact of a simple control strategy, on the contrary, is considerable, regardless of the tank size. Results of this study are presented in Chapter 5, since they mainly concerns the applied control strategy.

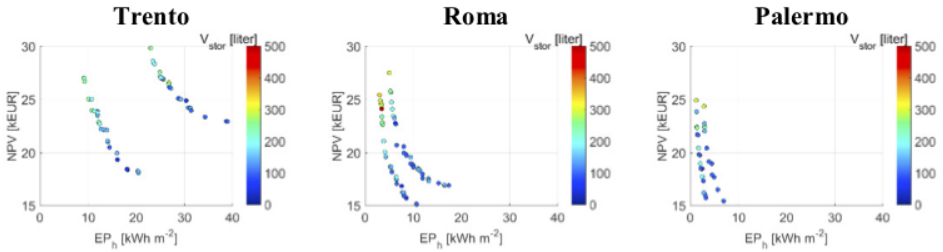

Figure 3.10: *Dominant solutions (Pareto front) obtained with the optimisation by minimizing the net present value (NPV) and the energy performance of the building (EP). The color scale highlights the optimised storage volume, V_{stor}. The lower curve refers to the high performance building, whereas the other curve to an average performance building.*

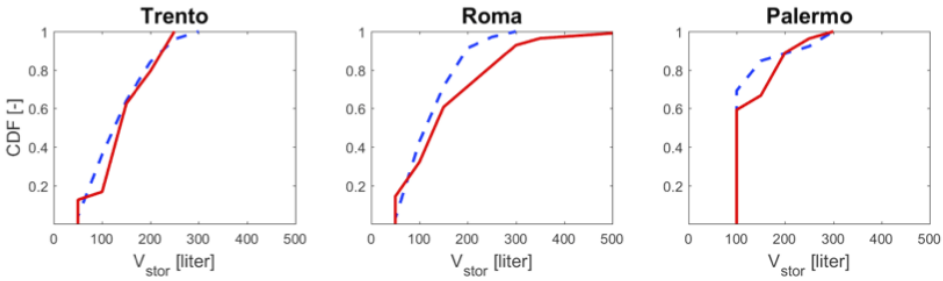

Figure 3.11: *Cumulative distribution function (CDF) of the water storage volume, V_{stor}, in the Pareto solutions shown in Fig. 3.10. The solid red line is referred to the high performance building, whereas the dashed blue line to the average performance building.*

CHAPTER 4

Analysis of the climate influence

Air-to-water heat pump systems, coupled with PV panels, are strongly influenced by the specific climate regime. In particular, both the air temperature and the solar irradiance have the most relevant impact on the behaviour of those systems, since they have a multiple influence on it. The air temperature has an effect on the building thermal losses, HP efficiency, and PV efficiency, while the solar radiation affects the building solar gains and the PV power production. (Harkouss et al., 2018) stated the importance to separately treat each climate so as to correctly design high performance building systems, since the best strategy to reach the nZEB target is deeply depending on that.

The study reported in Paper 8 extensively discusses the behaviour of PV

Figure 4.1: *Location of the European cities considered in the analysis.*

and air-to-water HP systems for residential heating and cooling. This analysis is performed in different cities across Europe, distributed over a wide range of latitude, as shown in Figure 4.1. Specifically, the cities considered in this analysis are Helsinki, Stockholm, Copenhagen, Berlin, Strasbourg, Milan, Rome, Palermo, and Athens. Since this technology is suitable for adoption in climates that show very different characteristics, it is important to appreciate that the annual behaviour and the energy balance of such a system undergoes substantial variations from place to place, as assessed in Paper 8. It is also worth noticing that, in this study, the DHW does not need to be considered and it is assumed to be covered by a separate dedicated production system, although it is possible to produce DHW by means

of an integrated system (*i.e.*, with the same generation system). There is a two-fold reason behind this assumption. On the one hand, the objective is to clearly show the impact of the climate, which is emphasized when the only needs of the building are heating and cooling; on the other hand, the choice is supported by the fact that, based on the principle of nZEB, as defined in the EPBD recast directive (European Union, 2010) there has been a trend of the designer to move from conventional systems based on mono-carrier/mono-converter solutions to a multi-carrier/multi-converter to cover the energy loads, (Fabrizio et al., 2014). Numerical analyses were performed considering the coupled simulation of a single-family house, as introduced in Section 2.2.2, and its energy system. This environment is set up in the TRNSYS simulation suite, using standard and TESS libraries to model the building and HVAC components.

4.1 Variations of the heating and cooling needs

In this Section, the heating and cooling energy use is analysed. Notably, the amount of energy related to heating and cooling needs of average buildings mainly depends on the properties of the opaque envelope and on the climate. In general, the heating load is more impacted by thermal transmittance with respect to the cooling load, whereas the thermal inertia has a greater impact on the cooling demand (Di Perna et al., 2011). However, it is also worth highlighting that (Goia et al., 2015) stated that the impact of the thermal transmittance on the cooling demand is not negligible.
In the proposed analysis, the only difference between the two types of modelled buildings is in the value of the transmittance of the opaque envelope. Depending on the climate region, and excluding the warmest locations (namely Athens and Palermo), the renovated building (RB) has a larger

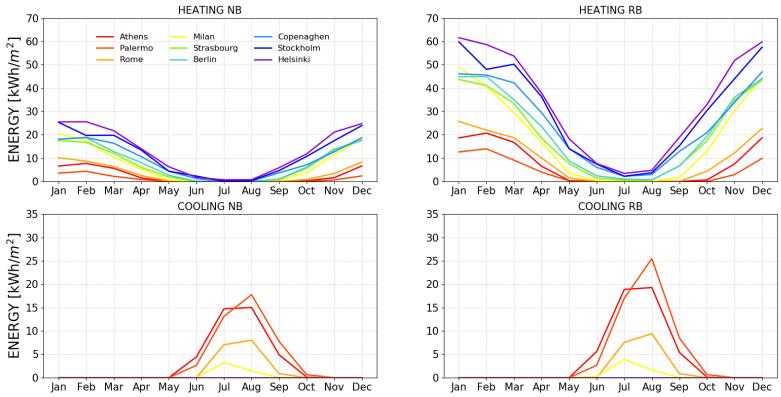

Figure 4.2: *Heating and cooling energy use (monthly values) for both the buildings with wall thermal trasmittance of 0.25 W· m^{-2}· K^{-1} (new building, NB) and 0.5 W· m^{-2}· K^{-1} (renovated building, RB).*

heating demand with respect to that of the new building (NB); in particular, the RB demand is between 2.3 and 3.3 times that of the NB. In a similar way, the RB cooling demand can be up to 1.3 times larger when compared to that of the NB. The graphs provided in Figure 4.2 report the monthly energy use for all of the considered cases.

4.2 Self-consumption potential across Europe

Self-consumption, as defined in Section 2.3, is hereafter expressed in terms of annual energy. The remaining percentage of the PV production is denoted as energy input to the grid (GI, or grid input). In Paper 8, the PV area is dimensioned in order to fit the available space on the roof facing south (referring to the building in Figure 2.1). Neither the area nor the tilt

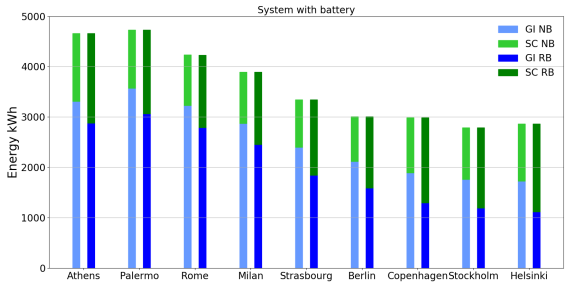

Figure 4.3: *Yearly energy shares of Self-Consumption (SC) and Grid Input (GI) for the case with the battery and for both the new building (NB) and the renovated building (RB).*

angle are changed depending on the climate. Due to the fact that other appliances were not taken into account in this analysis, the PV production surplus (*i.e.*, the energy input to the grid) seems to be quite large; the PV array area would not result oversized if other electrical appliances were included.

As shown in Figure 4.3 the total annual SC does not vary significantly when moving from warm climates to colder ones. On the contrary, its yearly distribution is significantly impacted by the specific location and it depends on both the availability of solar radiation and the load distribution.

In Figure 4.4, the monthly values for Palermo, Strasbourg, and Helsinki are compared so as to obtain further insight on this aspect. It can be noticed that there is a substantial increase of the self-consumption for the system that includes the battery.

The histograms reported in Figure 4.5 basically show the net PV production, which is composed by the sum of the self-consumption and the energy fed to the grid (SC+GI). An increase in the water storage volume (from 50

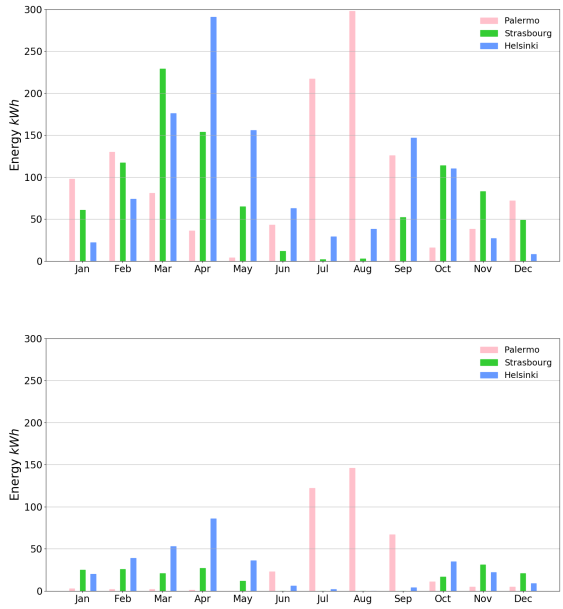

Figure 4.4: *Monthly Self-Consumption for three cities with very different climate for the cases with (above) and without (below) battery and for the new building.*

to 200 liters) does not yield a significant variation of the self-consumption, but only to a slight increase of the energy need for larger tanks, due to the increased thermal losses. The motivation behind this behaviour is given by the basic control logic, since it is not aimed at taking advantage of the thermal inertia, (Fischer et al., 2016, 2017).

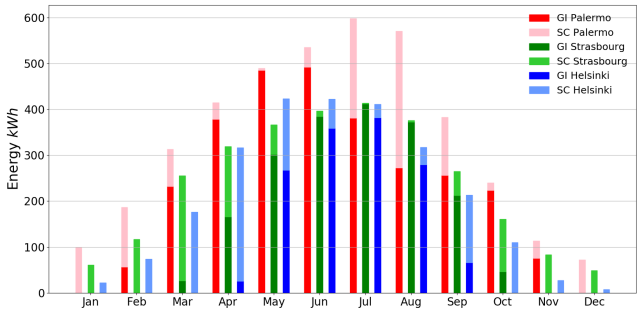

Figure 4.5: *Monthly energy share of Self-Consumption (SC) and surplus energy (grid input, GI) for three reference cities: Palermo, Strasbourg, and Helsinki.*

4.3 Self-sufficiency potential across Europe

Figure 4.6 shows that the self-sufficiency ratio (SSr, the share of energy need covered by means of solar energy, as defined in Section 2.3), can reach annual values higher than 90% for the high performance building (NB) with a battery (useful capacity 12.5 kWh) in warm climates (Athens, Palermo, Rome), while it is only 20% in Helsinki. When observing the building with lower performance (RB), the share covered by means of solar energy is still quite large for Athens and Palermo, whereas it is approximately 65% for Rome and it is significantly lower for the other cities. The solar covering fraction is lower than 10% for both buildings when considering PV systems without battery in mild and harsh climates (*i.e.*, Milan, Berlin, Copenhagen, Strasbourg, Helsinki, and Stockholm).

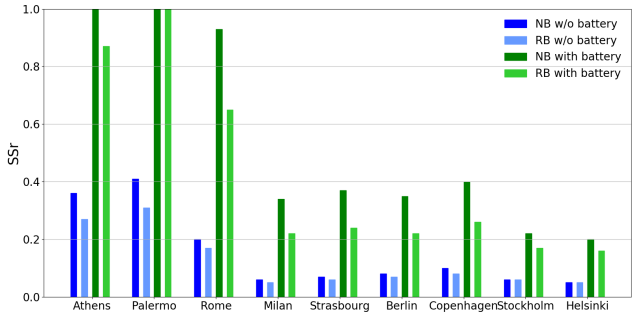

Figure 4.6: *Yearly self-sufficiency ratio (SS_r) for the system with and without battery and for both the new building (NB) and the renovated building (RB).*

4.4 The impact of boundary conditions

As already mentioned in the introduction, the analysed system, when compared to traditional systems (boilers), is more influenced by boundary conditions. The outside temperature deeply impacts the HP performance and the building losses. On the one hand, well insulated buildings are less affected by outside temperature variations; on the other hand, they are more influenced by solar gains and internal gains (and by the occupants' behaviour, in general). Finally, by adding the PV component, the solar radiation gets a greater impact on the system, especially on the final (net) energy use. In another study, which focuses on the prediction of the energy demand, a selection procedure is addressed in order to understand which features are actually having an impact on the demand. The aim of the selection procedure is two-fold: i) avoiding information redundancy, which can arise due to potentially high correlations among different features; and

ii) reduce the model complexity. The procedure implemented to reduce the number of features is known in the literature as *stepwise regression*, which relies on the computation of a specific metric to measure the significance level of a feature. Backward elimination is then applied by exploiting the p-value (or observed significance level): large p-values denote features that are not good predictors, which are thus eliminated. At the beginning, all of the features are kept into the selection procedure and provided as input to the multiple linear regression model; for each single feature the p-value is computed and the feature corresponding to the largest p-value is eliminated. The model is then re-fitted without the eliminated feature and the above procedure is repeated. The iterations proceed until all of the remaining features have a p-value lower than or at most equal to a predefined threshold, set to 0.1 in this analysis. As an example, by implementing the backward elimination procedure to select the most relevant features only, the relative humidity was removed from the regression model as, based on its p-value, it resulted to be a poor predictor of the consumption. From a preliminary analysis, by means of the outside temperature, the solar irradiance, and the internal gains due to people presence, it is possible to correctly model the energy consumption of the considered system. However, this is not the main focus of the above mentioned study, which is presented in details in Chapter 5.

CHAPTER 5

Control strategies

5.1 The need for enhanced control strategies

The analysed HP system combined with a PV (grid connected) system can help increasing the autonomy of the householder from the electricity provider. The extent to which the total electrical load can be matched by the electricity produced on-site is highly affected by the adopted control strategy, consisting of an algorithm which can be more or less sophisticated. Due to the decreasing trend of the electricity tariffs fed into the grid, many recent studies have proposed various approaches to increase the self-consumption share of the electricity produced by the PV system. This goal typically goes along with another objective: a reduction of the peak of power

fed to the grid. In the extensive review by (Luthander et al., 2015), results from several studies on this topic have been gathered focusing on different aspects (*e.g.*, behavioural responses to PV, demand side management or energy storage, both electrical and thermal). (Salpakari and Lund, 2016) applied a rule-based control to a residential case study with the objective of both reducing the cost and maximizing the self-consumption. Those objectives are shown to be achievable, but it is worth noticing that the considered system includes a battery. Thermal energy storage is significantly less expensive than batteries and a certain amount of thermal storage capacity is typically foreseen in domestic systems, (Facci et al., 2018); for example, a water storage tank for DHW is common. Moreover the structural thermal mass of the building has a great potential of load shifting, as shown, for instance, by (Reynders et al., 2013; Uytterhoeven et al., 2019). The capability of the building system to use electric energy when it is convenient (and not when needed by default) is typically referred to as flexibility. The flexibility potential is given by either the storage capacity and/or programmable appliances. The latter is not studied in this thesis, but it is indeed a viable solution and it has been studied by other authors (for instance (Salpakari and Lund, 2016; D'hulst et al., 2015; Widén, 2014). Control strategies are fundamental to activate the flexibility and exploit it in order to achieve the desired objective (*e.g.*, cost minimization, self-consumption maximization, peak reduction, etc.). A method to rate the flexibility by means of an indicator is proposed in (Arteconi et al., 2019).

5.2 Overview on the analysed control strategies

The most straightforward type of control is based on pre-defined rules, which are typically referred to as *rule-based algorithms*. Other authors have

proven the effectiveness of this kind of control strategies, despite their simplicity, for instance (Clauß et al., 2019; De Coninck et al., 2014; Tam et al., 2019). In the studies presented in this chapter the focus is mainly on rule-based algorithm. Paper 3 investigates whether the sizing of the water storage tank and the control applied on it can impact the self-consumption share and, consequently, the renewable share of the used primary energy. The study involves four different European climates and two types of building envelopes with different thermal capacities (timber and concrete). The most relevant outcome of this study is that the proposed control algorithm can increase the self-consumption, while increasing the water storage volume without any particular control does not impact it. The control logic is simple but effective: it sets a higher temperature in the tank when self-produced energy is used (batteries discharging or directly from the panels). In Paper 4, energy management algorithms that utilize weather and electricity price forecasts are evaluated, with the objective of minimizing the annual cost of purchased electricity by using the thermal storage of the building, the hot water tank, and electrical storage. The investigation is performed in a scenario with a modern single-family house with exhaust air heat pump located in Sweden. In Paper 6, simple control strategies based on the actual PV generation and the outdoor temperature are developed for shifting the demand, by taking advantage of the total storage capacity of the system. The objectives are to reduce the peak power taken from the grid and to increase the self-consumption of the solar energy. In this study, the context is that of a single-family house, equipped with a radiant floor and an air-source inverter-driven heat pump for SH and DHW preparation, which is also the same scenario used in Paper 7. However, in the latter study, the control algorithm is based on the hourly electricity tariff, which is assumed to be known in advance. The tariff is used as an input

data to take decisions on the HP control, by running the unit at a higher capacity (*e.g.*, by increasing the set point) when the electricity price is low, and storing energy to be used when the tariff rises. In Paper 9 a scenario similar to the one in Paper 4 is considered as baseline case. It involves both real-time control approaches and control logics that use forecast services in the near horizon (for weather and electricity price data); moreover, the system is analysed both with and without electric storage. In Paper 10, another rule-based control strategy, based on the instantaneous PV power production, is developed with the purpose of enhancing the SC. This strategy exploits the building's thermal capacitance as a virtual battery and the thermal storage capacity of the system by running the HP to its limit when PV surplus power is available, and by eventually using an electric heater in order to reach higher temperatures. The context of application is a single-family house (the one already described in Section 2.2.2 and used for other studies as well) in a climate typical of northern Italy, in which the Italian net-metering scheme for the power generated by on-site PV plants is applied.

Finally, an additional aspect related to the control has been addressed. Two methods to predict the energy demand are compared to each other. Predictions on the electric demand of the building and its system can be exploited to optimize its control, by means of either simple (*i.e.*, deterministic) or more advanced (*e.g.*, model predictive control) algorithms. In addition, it can also bring benefits to energy management at district level. At the end of this Chapter, a control strategy based on the demand prediction is proposed.

In the next sections, the studies are presented in details and organized according to the type of input that the algorithm receives in order to take decisions. The input can be an instantaneous variable (*e.g.*, derived from

local measures) or relative to the near future (*e.g.*, forecast service). In both cases, the input is deterministic with respect to the system, meaning that it does not depend on its behaviour. A third type of algorithm analysed in this thesis is the non-deterministic one; in this case, the decisions taken to control the system depend on the behaviour of the system itself.

5.3 Control algorithms based on instantaneous values

The most straightforward type of control is based on pre-defined rules, which are typically referred to as *rule-based algorithms*. The approach used in Paper 3 is aimed at increasing the self-consumption. In the reference case, the temperature of the water supplied to the radiant floor is controlled by means of a set-point on the thermostat signal (20°C, with proportional band of ±0.5°C) and the mass flow varies linearly between 100 and 400 kg h^{-1}. The HP is modelled by means of the TC model discussed in Chapter 2 and, therefore, it is controlled by the set-point for the supplied water. Moreover, the set temperature for the reference case is changed according to the outdoor temperature, a typical setting in heating systems (it is usually referred to as outdoor temperature reset, OTR, or climatic curve).
The proposed control logic considers a constant set temperature of 38 ° C (tank set point, *i.e.*, supply temperature to floor heating) when the electric energy is coming from the grid and a higher temperature (45 ° C) when PV energy is used (*i.e.*, discharging batteries or directly from the PV modules).

The control system ensures an indoor temperature between 19.5°C and 23°C and it significantly reduces the use of energy from the grid in all the simulated cases, also with a small water storage tank of 300 litres. This study is also referred to in the section on the component size (see Chapter 3), since simulations were performed for five tank sizes (in the

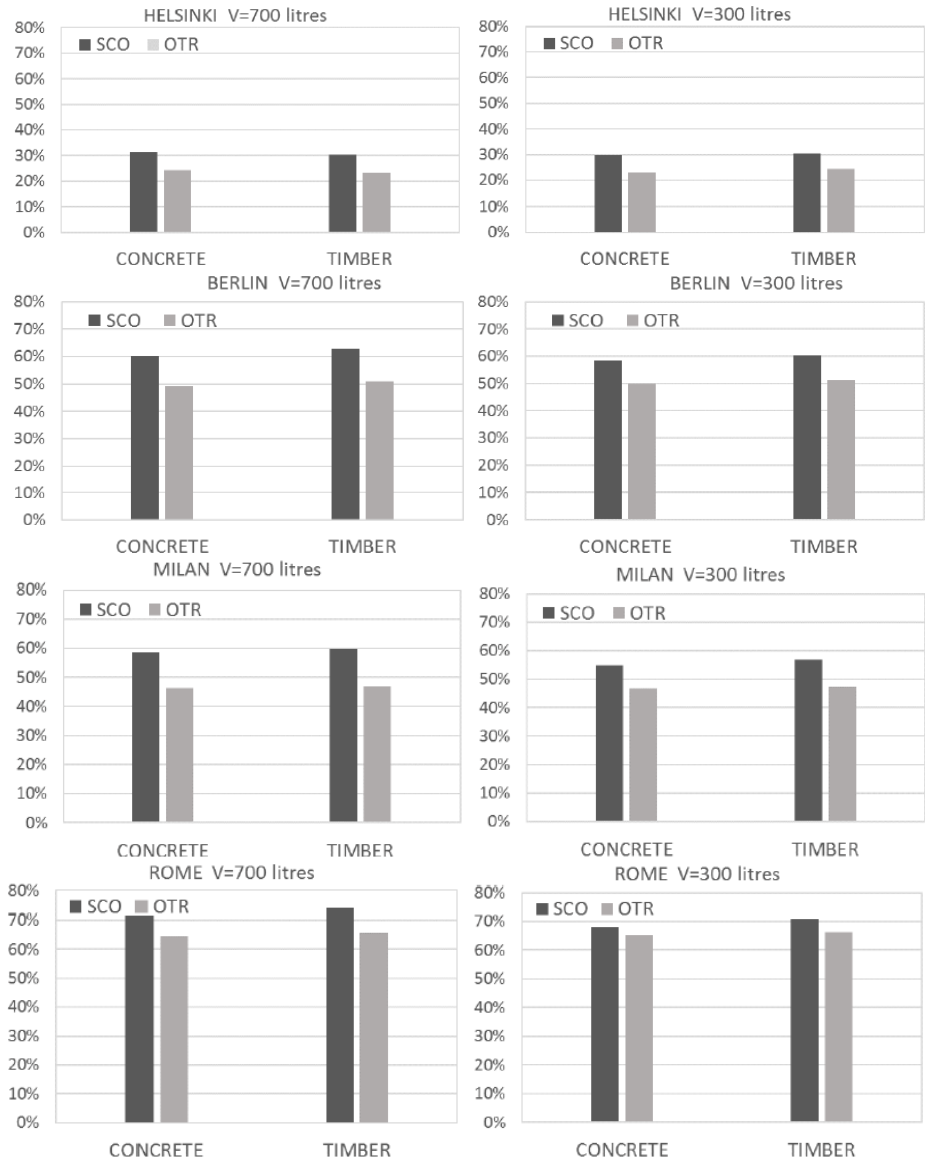

Figure 5.1: *Self-Consumption (SC) percentage of the SC-oriented (SCO) and Outdoor Temperature Reset (OTR) functions, with* 300 *and* 700 *litres tank volume equal,* 4 *climates, and the* 2 *envelope types.*

Table 5.1: *Set-points configuration for the different control strategies.*

Description	**Input signal**	**Set-points variations**		
		DHW Tank	**SH Tank (heating curve)**	**Ambient**
Reference case	-	0	0	0
Test 1	PV	$+7/-3$	$+2/-2$	$+2/-1$
Test 2	OT	$+7/-3$	$+2/-2$	$+2/-1$
Test 3	PV and OT	$+7/-3$	$+2/-2$	$+2/-1$
Test 4	PV and OT	0	$+2/-2$	$+2/-1$
Test 5	PV and OT	$+7/-3$	0	0
Test 6	PV or OT	$+7/-3$	$+2/-2$	$+2/-1$

OT: outdoor temperature.

range between 100 and 1000 litres), besides for the four climates and the two types of envelopes. However, increasing the storage volume results in having a lower impact on the self-consumption with respect to the application of the control algorithm, as shown in Figure 5.1.
Also in Paper 6 the control strategy is based on instantaneous variables; in particular, on the actual PV generation and the outdoor temperature. At every time step of the simulation, a function (PV function) checks if there is PV power available; another function determines whether the outdoor temperature is high or low with respect to the daily temperature oscillations by comparing it with the average temperature in the last 48 hours. On the base of these two functions, independently or combined together (as shown in Table 5.1), the set-points of the DHW tank, the SH tank, and ambient thermostats are increased or slightly reduced. In this table, a summary of the four analysed configurations is provided.

In this analysis, the set-point variations have been selected aiming at not causing significant perturbations to the comfort of the occupants. Thus, the maximum value of the ambient set-point is 22°C and the minimum is

set to 19°C (the default value is 20°C); the DHW tank temperature has a baseline case of 48°C and it is set to a value in the range between 45°C and 55°C by the control function. The SH tank temperature does not have a direct effect on the comfort of the occupants, since the system also controls the mass flow to the underfloor pipes. However, a limited increment (+2°C) can be accepted without risking any floor overheating, considering that the supply temperature is given by a heating curve with a maximum equal to 35°C.

The key parameters to evaluate the performance in this study are the electric energy use, which is the sum of the self consumption (SC) and the energy drawn from the grid, both on a monthly and a seasonal basis. When the control functions are applied, there is an increase in the self-consumption and a decrease in the energy drawn from the grid. The larger increase in SC (compared to that of the reference case) arises in Test 1: in this case, it is 61% of the total consumption, compared to 14% in the reference case. The best case in terms of reduction in the energy drawn from the grid is given by Test 3: here, there is a reduction from 86% of the total energy use to 33%. Since the total energy use can significantly vary, the solution that minimizes the grid energy is not always the same which is maximizes the self-consumption. In Figure 5.2, the green dashed line represents the points for which the sum of the x-axis and y-axis values (*i.e.*, the total consumption) is equal to the consumption of the reference case; the points located below the line (Test 1, 3, and 4) have a lower total consumption while the ones above the line (Test 2, 5, and 6) have a higher consumption. In both Test 1 and Test 3, all the set-points are modified and the PV function is applied. With respect to the monthly values, a two-sided effect can be observed on the total energy use (*i.e.*, the sum of the energy drawn from the grid and the PV production): on the one hand, the total consumption

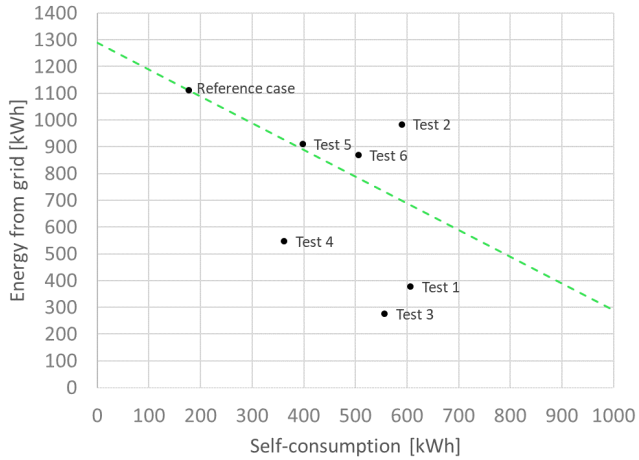

Figure 5.2: *Combinations of seasonal Self-Consumption and drawn energy for all the simulations. The green dashed line represents a total consumption equal to the one in the reference case.*

is reduced in cold months (*e.g.*, January), while, on the other hand, it is incremented in months presenting a low heating need (*e.g.*, October). This behaviour can be motivated by observing that, in October and April, there is a low heating demand, which increases because of the set-points increase: the stored energy that is not used, it is lost. In January, the heat pump can operate with better performance due to the shift of the demand to hours corresponding to higher outdoor temperatures.

Since the algorithms used in Test 1 and 3 provided better performance, the PV function seems to have a grater impact than the function based on the outdoor temperature. Therefore, the PV function has been further developed in Paper 10. A new control strategy (HP+) is proposed as a further development of the algorithm based on PV production. The HP+ algorithm

first checks the AWHP capacity and compares the available PV power with the minimum and the maximum power absorption of the AWHP. The set-points are therefore increased proportionally to the excess PV power: the maximum set-point variation is applied when the PV production is greater than the HP power absorption at the maximum speed. Otherwise, only a fraction of the maximum set-point variation is applied as in the following equation:

$$T_{set,HP+} = T_{set,ref} + \frac{T_{set,max} - T_{set,ref}}{P_{abs,max} - P_{abs,min}} \cdot \max\{0, P_{PV,surplus} - P_{abs,min}\} \tag{5.1}$$

where: i) $T_{set,ref}$ and $T_{set,max}$ denote the reference and maximum set-point temperatures; and ii) $P_{abs,min}$, $P_{abs,max}$, and $P_{PV,surplus}$ denote the absorbed powers (minimum and maximum), and PV surplus power. The set-points are never reduced but only increased, with the purpose of avoiding any possible discomfort (even if acceptable, like in the previous study). In this way, the algorithm can be more easily compared with the reference case, since the same indoor conditions are maintained. The maximum set-points is 55°C for the water tanks (the maximum temperature supply of the AWHP) and 22°C for the room temperature. Moreover, an additional function (EH+, electric heater plus) is implemented to activate the electric heater signals . This new function checks if some PV excess is still available after the maximum temperature that the HP can provide (55°C) is reached in the tanks. In this case, the excess power is used to heat the DHW storage to a higher temperature (up to 90°C) by means of an electric heater (two subsequent stages of 500 W depending on the available excess power). This strategy is aimed at maximizing the self-consumption of the PV production. However, it has the drawback of a high exergetic cost due to the use of the electric resistance, which affects the second-law efficiency

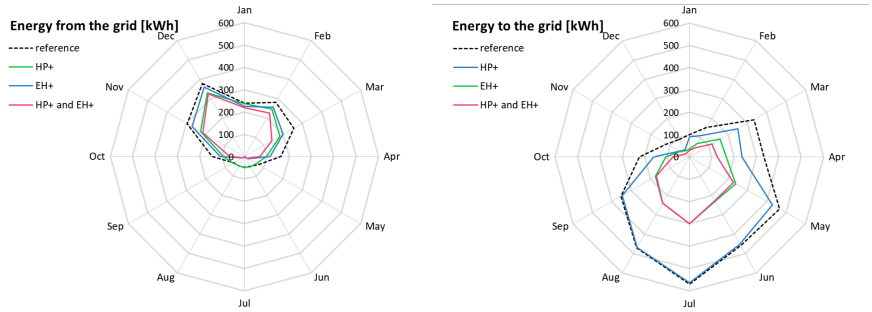

Figure 5.3: *Monthly energy exchanges with the grid for the reference case (dashed black lines) and for the three cases (solid lines) in which the control algorithms are applied (PV area 20 m^2).*

of the system. The HP+ and the EH+ functions are applied either independently or in combination (HP+ and EH+), with priority for the HP+; the results of the three simulations with the control strategies compared to each other and to the reference case are shown in Figure 5.3 in terms of monthly energy fluxes. All of the applied algorithms have the effect of reducing the exchanges with the grid (energy drawn from the grid and energy fed to the grid). Basically, both the SC and the SS are increased by the control algorithms; this happens in particular when HP+ and EH+ are combined: in this scenario, there is an increase from 7% to 60% in the SC_r and an increase from 12% to 65% in the SF. This behaviour remarks the benefits which the grid manager can obtain in case these algorithms were extensively implemented in buildings with PV systems. Another observation is that the reduction of the energy fed to the grid is more evident than the reduction of the energy drawn from the grid, which means the total consumption is higher with the control strategy.

In Paper 9, two control strategies (out of six) are based on instantaneous

values (of available PV power), while the remaining are based on foreseen values. The first algorithm acts on the thermal storage, whereas the second acts on the electrical storage (battery). In the **thermal storage mode (TH)**, the aim is to overheat the living room and the bathrooms above their reference set point (21 and 22°C, respectively) and to overheat the DHW tank above its reference set point of 50°C, on the basis of a minimum threshold of PV excess equal to 320 W. When this mode is active, the speed of the heat pump compressor is modulated so that the absorbed power roughly matches the available excess PV electricity (some limitations are due to the time response and minimum speed of the compressor). The compressor frequency $f(HP)$ is based on the evaporator and condenser temperatures (T_{evap} and T_{cond}, respectively), and the excess PV available electricity (PV_{exc}), as shown in the following equation:

$$f_{HP}(PV_{exc}, T_{evap}, T_{cond}) = a_1 + a_2 PV_{exc} - a_3 PV_{exc}^2 + a_4 T_{evap} - \\ - a_5 T_{evap}^2 + a_6 T_{cond} - a_7 T_{cond}^2 + a_8 T_{evap} T_{cond} \tag{5.2}$$

During overheating, the backup auxiliary heater is forced to be inactive. In the **electrical storage mode (EL)**, the battery charging occurs when there is an excess PV production, after the domestic appliances load is met. The discharging occurs when the total electric load exceeds the PV production. The state of charge range is between 10 and 90%. If both thermal and electrical storage are active, the thermal storage has the priority and the battery is only charged after the (raised) set point is achieved or the excess PV is greater than power absorbed by the HP, so that the battery can be charged at the same time. In other words, it is possible to activate the TH mode or the TH+EL mode, but not the EL mode only. The KPIs derived from the application of TH and EL are presented in the next section, in

which more advanced algorithms are discussed, to make a comparison.

5.4 Control algorithms based on electricity prices

Potential benefits obtained exploiting the knowledge of the price variations have been addressed in other studies. In the analysis reported in (Zhang et al., 2017), the battery adapts to the electricity price so as to store electricity when it is low and to provide it when the price is high; three HP control strategies were proposed by (Schibuola et al., 2015), exploiting the cost of electricity and on the photovoltaic power generation. In the study proposed by (Henze et al., 2004), the time-of-use price signal was exploited so as to shift the electrical loads to off-peak periods during the night and the weekends in cooling applications; another interesting analysis, with respect to cost reduction, is the one discussed by (Biegel et al., 2013). (Fischer and Madani, 2017) proposed a two-group classification for the various pricing schemes applied in heat pumps analyses: i) time-of-use prices applications, *e.g.*, traditional high-low tariff schemes that can be static over long periods; and ii) dynamic prices with daily changes (day-ahead pricing), or even shorted time periods (real-time-pricing).
Limiting the need of purchasing electric energy when it is expensive can help to reduce the bill for the householder, but it could also benefit the grid management by reducing the daily unbalance between the availability of renewable power and the demand. A possible action on the heating system based on electricity prices involves the storage system (thermal and, possibly, electric). Studies involving rule-based control using variable electricity prices approaches in different ways the definition of high and/or low price. (Schibuola et al., 2015) defines fixed price thresholds for the whole year. In (Coccia et al., 2018) the hourly price variation is divided by the

maximum hourly variation in the year an this ratio determines a variation on the set-point. (Clauß et al., 2019) defines high and low price thresholds for the 24 hours ahead. This ensures that every day there are both high and low price periods (unless the profile is flat) and it uses only available information (the day-ahead hourly price is typically known, whereas the evolution along the year is not predictable). Also the approach used in Paper 9 uses available information and it is a robust method as it does not depend on the price general trend. Here, the price is defined as high or low not in absolute terms but by comparing the current price with the running average price in a near-future interval of time. In other words, the price is considered low or high relatively to what happens in the hours ahead. Figure 5.4 explains the logic that determines whether the current price is low or high; the grey/green intervals correspond to the hours in which the price is high/low (*i.e.*, higher/lower than the upper/lower limit). The width of the interval in the future used for the moving average is an adjustable parameter.

The day-ahead spot market data are obtained by using a perfect forecast, which is derived from the same input file of electricity price data, shifted one day ahead. The upper and lower limits are equidistant from the running average calculated on a interval in the near future. Therefore, the so defined high price signal has the meaning that the price is going to decrease and vice-versa for the low price.

To examine the impact of higher daily oscillations of the price, which could be the case in a future scenario, the data from 2015 is amplified by applying a factor of 2 to the deviation from the 24 hours running average, as explained in section 2.2.4. Results from applying control strategies based on the dynamic electricity price are presented both in Paper 9, which is the continuation of the study presented in Paper 4, having a Swedish scenario,

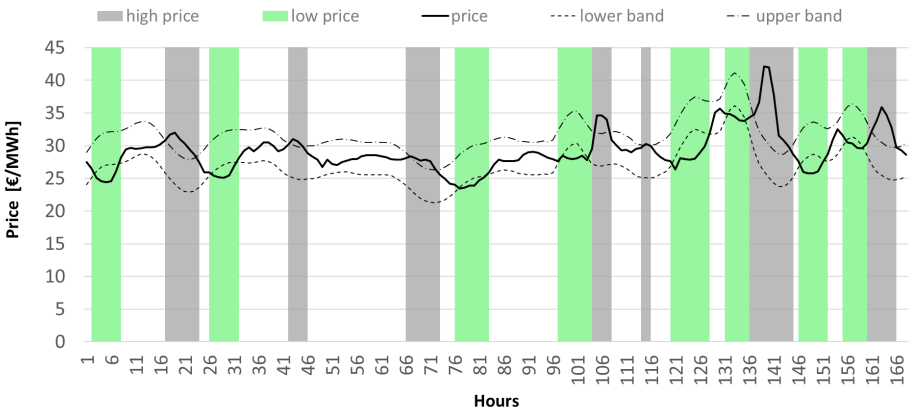

Figure 5.4: *Example of high price periods (data from a week in Jan. 2015). The grey dashed lines show a backward shifted moving average of the price signal (solid black line) that are used to identify the high and low price intervals.*

and in Paper 7, which refers to an Italian context.

In the studies regarding Sweden, both variable monthly tariffs (flexible tariff scenario) and dynamic hourly spot market prices are considered (Swedish Energy Agency, 2018). Based on the low-price and the high-price signals, the room set point is raised by 0.5 K and lowered by 0.5 K, respectively. However, there are some limitations in order to prevent discomfort and avoid unnecessary use of the backup electrical heater. It is not allowed to reduce the zone temperature set point when daily average outdoor temperature drops below 0°C and it is not allowed to overheat the zones when the daily average temperature exceed 10°C. The PRICE mode can be activated if the above mentioned TH mode is also active and the algorithm is called **PRICE_TH** (please refer to Table 5.2 for an overview of the algorithms applied in the Swedish scenario). In the case that TH mode occurs at the

Table 5.2: *Control strategies overview for the Swedish scenario.*

Simulation case	**Input signal**	**SH setpoint**	**DHW setpoint**
Base case	-	Ref	Ref
TH	Instantaneous PV	$+1^{\circ}C$	$+6^{\circ}C$
PV_TH	Weather forecast	$+1^{\circ}C$	$-5/+6^{\circ}C$
PRICE_TH	Price forecast	$\pm 0.5/+1^{\circ}C$	Ref/$+6^{\circ}C$

The scenarios *Base case+EL, TH+EL, PV_TH+EL, PRICE_TH+EL* differ from the others for the presence of batteries and for the priority given to charging.

same time as PRICE mode, the room set point is raised by 1.0 K in addition to the PRICE setting and the set point for DHW is raised to 6 K above the reference value. In the scenarios with a battery, the EL mode can also be activated and the algorithm is therefore called **PRICE_TH+EL**. The priority is still the same, *i.e.*, satisfying the appliances load, overheating, and, finally, charging the battery, in this order.

In Paper 9, simulations are run with three different PV sizes, each with an accordingly sized battery (3.1 kW PV and 3.6 kWh battery, 5.7 kW PV and 7.2 kWh battery, 9.3 kW PV and 10.8 kWh battery). For the specific price boundary conditions of Sweden (which are described in Section 2.2.4), the PRICE_TH algorithm results in relatively small cost savings, compared to other proposed algorithms. A possible reason is that the dynamic spot market price contributes for only a third of the total end user electricity bill in Sweden, and the oscillations are small compared to those of other European countries. In order to verify how the performance of the control strategy is affected by the price variation, the oscillations have been amplified a factor of 2, as already explained above. Using the amplified profile, PRICE_TH leads to a higher potential of cost savings (up to 6%) for the system with the medium and larger PV systems, as shown in Figure 5.5. (Rodriguez et al., 2018) showed that around 13% cost savings could be achieved by

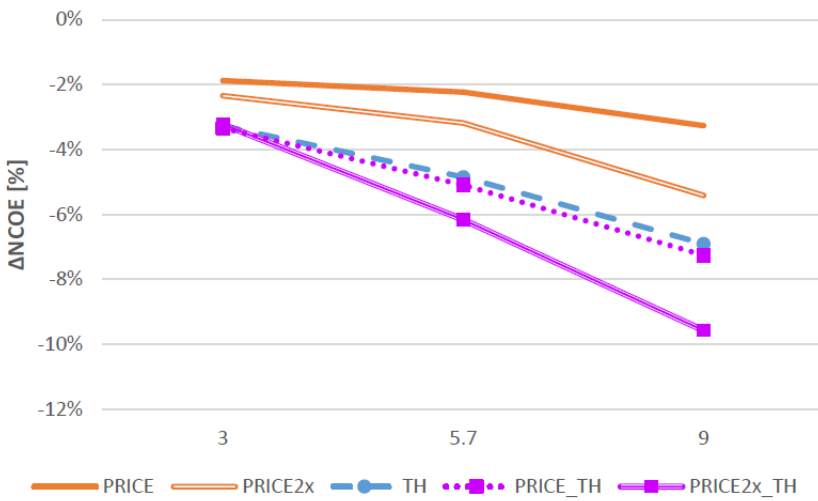

Figure 5.5: *Variation of the net cost of electricity (NCOE) for the householder compared to the reference cases with or without batteries, and for the three PV sizes, for the control modes: PRICE_TH for both real price variations and for amplified price variations (PRICE2x_TH), as well as pure thermal mode (TH) and the price based control on its own without overheating, for real price variation (PRICE) and amplified price variations (PRICE2x).*

applying a price-based control strategy, without sacrificing noticeably the thermal comfort. Their case study refers to a ground source heat pump in Germany, which is activated only if the price is below the average of the current day and the space heating set point temperature can deviate ±1K. As the absolute price variation in (Rodriguez et al., 2018) is more than twice what is used in this study, the results are quite consistent with the findings of this study.

Results of both PRICE_TH and PRICE_TH+EL are shown at the end of this section in Figures 5.7 and 5.8, in which they are also compared with

other algorithms. Figure 5.7 shows the variation of final energy (ΔFE) compared to the reference case (with or without batteries) for all control algorithms and for the three different PV system sizes. ΔFE increases with increasing PV system size, but the change is small between the medium and large sizes. The exception is for the PRICE_TH+EL case, which shows the largest reduction of FE with respect to the reference case. When the EL mode is not active (TH mode and PRICE_TH), the price-based strategy leads to a insignificant difference in FE for all the PV sizes, whereas the PRICE_TH+EL algorithm shows a final energy saving considerably larger than the TH+EL, especially for the medium and the large PV sizes. In any case, there is a trend that the price base control modes have greater impact with larger PV system sizes. Figure 5.8 shows the variation in net cost of annual energy (ΔNCOE), for all the cases. As for the final energy, there is little difference in NCOE between the PRICE_TH and the pure TH mode. However, compared to the reference case, the reduction is $3-7\%$, increasing with increasing PV size. For the cases with batteries (EL mode active), the only exception is for the largest PV size. In that case by applying the price based algorithm (PRICE_TH+EL) reduces the NCOE more than applying the TH+EL control mode.

A similar approach is used in Paper 7, although in a different scenario (northern Italy climate and Italian electricity prices), in a system based on an AWHP without PV and with some differences in the price-based control algorithm. This study aims to investigate the potential money saving by means of a simulations analysis, both in the case of time-of-use electricity prices (TOU) and real-time prices (RTP) from the day-ahead market. The function that defines when the price is considered high or low is the same introduced in the previously discussed paper, *i.e.*, it compares the current price with the average price over an interval of hours ahead. This interval

is defined by its width (Δt) and the time ahead at which it is centered (t_{ahead}). The function is applied to both the TOU tariff and the RTP, with the parameter Δt set to 7 hours and 4 hours, respectively, and t_{ahead} set to 9 hours and 6.5 hours. When the signal indicates a high price, the set-points of DHW tank, SH buffer, and ambient thermostats are raised, whereas in the remaining time they are slightly decreased. The variations have been established with the objective of not considerably affecting the comfort for the occupants. Hence, the ambient set-point has a maximum of 22°C and a minimum of 19°C (the default one is 20°C), the DHW temperature is set to 48°C in the base case while it is incremented up to 55°C and reduced to 45°C by the control function. The thermal comfort is not directly affected by the SH tank temperature, as the the mass flow to the underfloor pipes is also regulated proportionally to the temperature difference between the ambient set point and the actual room temperature. Since the supply temperature follows a heating curve with a maximum supply temperature of 35°C, a small increment (+2°C) can be accepted without excessively overheating the floor.

As shown in Figure 5.6, the effect of applying the control algorithm depends on the month: for periods in which the required heating load is low and intermittent (like in October or April), raising the set-point temperature of the SH buffer tank is not convenient, since the stored thermal energy may not be needed after being produced, and consequently the only effect would be an increase of heat losses. Similarly, by increasing the ambient set-point temperature, the heating terminals are activated during periods in which they would have been turned off with a lower set-point. In cold months, on the contrary, changing the set-points leads to a reduction of energy use: this is due to the particular daily profile of the price that increases during the day time, when also the outdoor temperature is higher and, consequently,

the the AWHP operates with a higher COP. However, the main objective of the proposed algorithm is to reduce the cost of electricity. In the case of TOU tariff, the average unitary cost of electricity is always reduced when the function is applied (negative variations of the unitary cost of the kWh for all the months, from -4% to -7%). However, this variation is very low and not always leads to a real decrease of the monthly cost, because of the increased energy use. That means the effective cost reduction (that is -26% in January) is mainly due to the energy use reduction (-22% in January) and only in part to a lower unitary cost (€/kWh). For the case in which the RTP is applied, the results are quite different: the control function is able to reduce the cost only in January (-17% compared to the reference case); however, unlike the TOU case, this reduction is caused by a reduction of the unitary cost. This is explicable by looking at the RTP data in Figure 2.6: in January the two peaks occurring in the morning and in the evening are very high, and the control function is made to exploit this variation of price. In other months, those peaks are almost absent, and consequently the control function does not lead to a cost reduction. As for the whole heating season, in the TOU case the total cost variation is positive ($+5\%$), which means it is not convenient to apply the control function in all the months. On the contrary, if it had been applied only in December, January and February, there would have been a significant money saving (-12% with respect to the reference case). In the RTP case, January is the only monthly in which it is convenient to apply the function. A similar conclusion regarding a price based control rule whit dynamic prices is in (Clauß et al., 2019), who also pointed out that such a control is effective only in the cases of great daily price fluctuations. The amplitude of the fluctuations, however, are very different from one country to another and can also vary significantly between different days.

Figure 5.6: *Monthly electrical energy use and relative cost for the reference case and for the case in which the control function is applied for both the time of use (TOU) pricing and the real-time pricing (RTP).*

5.5 Control algorithms based on weather forecast

Weather forecasts information can also be exploited in the system control, as showed by (Fischer et al., 2016). In the study from (Thygesen and Karlsson, 2016), the proposed control strategy is based on an ideal short-term weather prediction for PV HP that use thermal storage in 2 sizes of DHW store; however, limited profitability is shown.

Paper 9 also concerns this type of control strategies. In particular, a perfect forecast of irradiance is used to calculate the cumulative PV electricity production in the near future horizon. In the simulation, the forecast is obtained by reading ahead in the same weather file which provides boundary conditions for the current current time-step. At night, the algorithm checks if the PV production exceeds 0.5 kWh between 7 and 8 a.m.; in case it does, the set point of the DHW storage tank is lowered by 5K between midnight

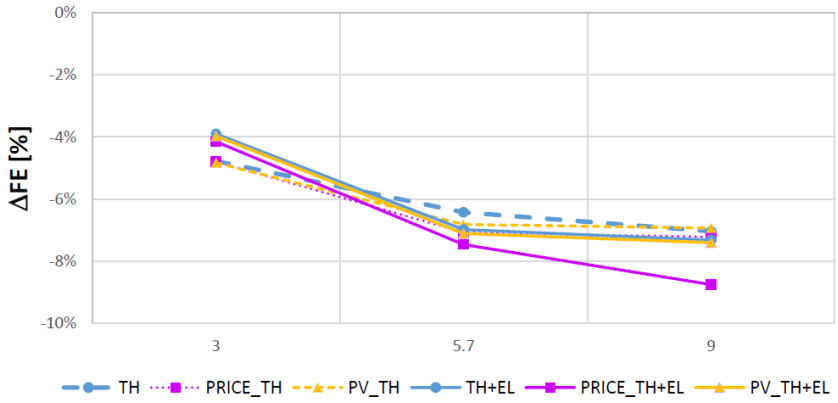

Figure 5.7: *Variation of the final energy (ΔFE) compared to the reference cases with or without batteries and for the three PV sizes, with or without batteries, for all control strategies.*

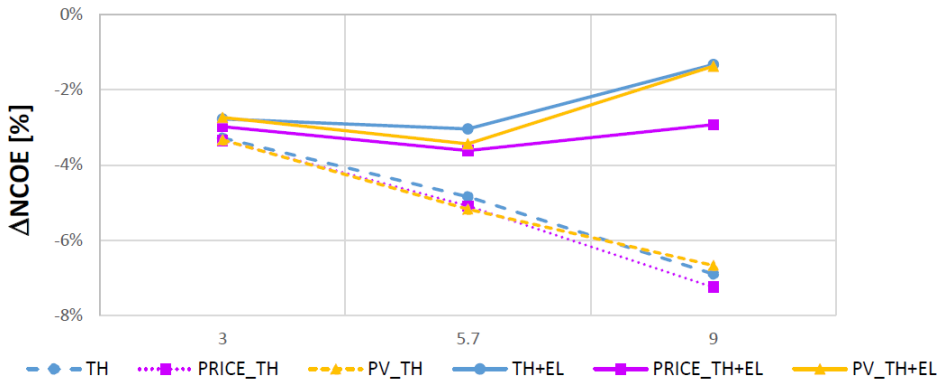

Figure 5.8: *Variation of net annual cost of electricity for the householder ($\Delta NCOE$) compared to the reference cases with or without batteries, and for the three PV sizes, for all control strategies.*

and 6 a.m.. This mode is combined with the purely thermal mode and it is therefore called **PV_TH**. The electrical heater is always disabled when overheating occurs. As for the price-based mode, in the scenarios with a battery, this control can be combined with the above mentioned EL mode. In that case it is referred as **PV_TH+EL**. Results are presented together with the previously discussed algorithms in Figures 5.7 and 5.8. The control based on the weather forecast shows a limited impact in all the cases. The maximum reduction of final energy in this paper is 7% without battery and 9% with the battery, compared to the reference case with and without electrical storage, respectively. The net annual cost for the end user is reduced by 7%, without battery. One of the main factors impacting the final energy and the cost is the activation time of the auxiliary heater: limiting its use for overheating is fundamental to have energy and cost saving. The demand of the auxiliary heater for space heating can be reduced by $24 - 43\%$.
A significant additional result lies in the almost doubled decrease of final energy and cost when a battery is included with respect to the case in which the proposed rule-based algorithm is added; moreover, the implementation of this control algorithm in the presence of a battery does not yield a reduction comparable to when no battery is present. A further result of this study is that, in Sweden, the selection of a contract involving dynamic pricing based on the spot market, yields money savings compared to standard contracts based on monthly average prices; this behaviour arises also when the algorithm that exploits price predictions (PRICE_TH) is not used.

5.6 Load forecasting for system control

When discussing Paper 7, one of the possible motivations behind the poor performance of the control algorithm in mid-season months, is that the

Table 5.3: *Summary on rule-based control strategies.*

	Applied rule	**Main findings on control**
Paper 3	Increase the supply temperature to floor heating when PV power is available (directly or from battery)	SC is increased, especially in warm climates, and the control function has more impact than any increase of buffer tank size
Paper 6	Increase/reduce DHW, ambient and SH supply SPs on the base of instant PV excess and outdoor temperature	All the algorithms are effective, especially those based on PV and that exploit all the thermal mass
Paper 7	Increase/reduce DHW, ambient and SH supply SPs on the base of day-ahead electricityprice forecast	The strategy is convenient only in the case of large price oscillations and in cold months
Paper 9	Increase/reduce DHW and ambient SPs on the base of day-ahead electricity price forecast, weather forecast and instant PV excess (HP power matches the excess power)	The presence of a battery yields to larger benefits than any rule-based algorithm
Paper 10	Increase DHW and ambient SPs with HP, proportionally to the PV excess and if PV excess is still available overheat DHW with electric heater	Strategies are effective in decreasing energy exchanges with the grid, but the Itaian net metering scheme discourage this behaviour

surplus thermal energy that is stored, if not needed afterwards, is wasted. This suggests that it would be interesting to know in advance the load of the building some hours ahead, in order to decide whether to store thermal energy or not, and consequently it highlights the necessity of predicting the load in order to better control the system. In this section, the focus is not on a particular control strategy but on the load forecasting, which can be used as input for control strategies (Zhou et al., 2008; Bacher et al., 2013). Control strategies based on an optimization and a prediction are typically referred to as model predictive control (MPC). However, some authors also refer to MPC whenever there is a predictive element in the control algorithm, although without any optimization process. The work by (Péan et al., 2019) provides a review on the analyses related to supervisory control aimed at improving energy flexibility for buildings in which heat pumps are installed. Despite the load prediction is only the first step in the development of a predictive control algorithm, it is not trivial to

obtain a good forecasting model. The growing interest for the consumption prediction in buildings is demonstrated by the surveys in (Amasyali and El-Gohary, 2018; Raza and Khosravi, 2015; Daut et al., 2017). Moreover, the prediction can also bring benefits to energy management at district level, especially in a scenario in which the majority of the house owners are prosumers (*i.e.*, they both consume and produce electricity). In this thesis, two methodologies for the prediction of the energy consumption of an AWHP system in a residential building are implemented. In particular, Multivariate Polynomial Regression (MVP) and Neural Network (NN) based regressions are analysed and compared to each other. With the selection procedure to identify the relevant features, discussed presented in Section 4.4, the outdoor dry bulb temperature and the global horizontal irradiance result to be the boundary conditions with a greater impact on the consumption, among those analysed. In addition, the heating water tank temperature, the ambient temperature (which are system state variables), the tank set-point temperature, and the ambient set-point temperature (which are control parameters) are used as predictors. The energy consumption prediction is performed covering n hours in the future starting from the current hour, *i.e.*, in hours $i, i+1, \ldots, i+n$ where i is the current hour. Therefore, the model shall consider both the current (known) weather variable (temperature and irradiance) and the weather forecast for the following n hours. The same applies to the control parameters to be set for the defined time horizon. Table 5.4 outlines the selected features and the relative time intervals used in the regression models.

Data pre-processing continues with the feature scaling process, which is performed by means of a standardization, in which each feature is rescaled so as to have the properties of a standard normal distribution. For the

Table 5.4: *Features (independent variables, IV) and prediction (dependent variable, DV): category, type, and time intervals.*

FEATURES (IVs)	**CATEGORY**	**TYPE**	**TIME INTERVALS (h)**
outdoor dry bulb temperature	Boundary condition	hourly average	$i, i+1, \ldots, i+n$
global horizontal irradiance	Boundary condition	hourly integral	$i, i+1, \ldots, i+n$
heating water tank temperature	System state variable	instant value (current time-step)	i
ambient temperature (mean of the 3 zones)	System state variable	instant value (current time-step)	i
tank set-point temperature	Control parameter	hourly value	$i, i+1, \ldots, i+n$
ambient set-point temperature	Control parameter	hourly value	$i, i+1, \ldots, i+n$
PREDICTION (DV)			
Total electricity consumption	-	Integral over n hours	$i, i+1, \ldots, i+n$

generic feature x, the standardized $\widehat{x}$ is:

$$\widehat{x} = \frac{x - \overline{x}}{\sigma_x} \tag{5.3}$$

where σ_x and $\overline{x}$ are the standard deviation and the mean of the generic feature x, respectively. This operation ensures that there is no feature dominating the others, since all of the features will have a similar range. Notably, to perform supervised learning algorithms, there is the need for two types of data sets: i) a training set; and ii) a test set. The former refers to the observations that are selected to actually fit and train the model, based on the expected (correct) output values; the latter refers to the input sequences that are fed to the model in order to evaluate its accuracy and correctness. Clearly, in order to properly evaluate the model and its stability, it is fundamental to test it on data different from that used in the training phase. It shall be noticed that a particular decision on how to split

the data into training and test sets might influence the performance of the method itself. In order to avoid such effect, *i.e.*, to obtain an evaluation not biased by the specific split methodology, a k-fold cross-validation approach is implemented. In this procedure, the full set of input sequences is split in k different groups: one group is selected as test set, while the remaining $k-1$ are the training set. The model is then fitted to this split, also known as batch, and its performance is evaluated. The procedure is repeated so as to use each possible combination of one test group and $k-1$ training groups and the average performance is obtained over all the batches; $k = 10$, which is a typical value in machine learning and artificial neural networks, was sufficient for the convergence of the performance score. All of the numerical analyses performed in this paper are evaluated with the k-fold method and are therefore not affected by a particular training/test split option.

Multi-Variate Polynomial (MVP) Regression Since the predicted value depends on multiple independent variables (features) and the dependency on each of them is not linear, the most intuitive regression model to be applied is the multivariate polynomial. The function describing the MVP regression is the following:

$$\begin{aligned} y = a_0 + a_{1,1}x_1 + \cdots + a_{P,1}x_1^P + \cdots + a_{p,m}x_m^p + \cdots + \\ + a_{1,M}x_M + \cdots + a_{P,M}x_M^P \end{aligned} \tag{5.4}$$

where P and p are, respectively, the maximum degree of the polynomial and the generic degree of a term in the polynomial, M and m are, respectively, the total number of features (independent variables) and the generic m-th feature in the polynomial, a_0 is the constant term (bias) and $a_{1,1}, \ldots, a_{P,M}$ are the coefficients of the terms of the polynomial.

Neural network (NN) Regression It shall be noted that the fitting performance of (5.4) is strongly impacted by the assumption of a polynomial dependency between the features and the predicted value. However, a more complex relation might subsist. Since the regression model does not need to describe the physical laws involved in the problem, while it is required to provide a computationally fast response, NNs provide an effective solution. Neural Networks are a widespread method, used in a wide variety of fields, which can be applied to regression problems, as discussed by (Goodfeloow et al., 2016); the NN is designed with an input layer composed by 22 nodes and the data standardisation reported in (5.3) is used as feature scaling approach. These nodes represent the input features shown in Table 5.4. Two hidden layers have been included in the network, each with 11 nodes, *i.e.*, the half of input nodes, which is a common initialization approach in NN. Both the hidden layers are composed by a rectified linear unit (relu) activation function (the function defining the relation between the node input and the node output, apart from the weights learned during the training phase), which, for a generic input value x, provides $y = \max\{0, x\}$ at its output. At the output layer, a single node is present since the goal is to predict the electrical energy consumption value, which is a scalar. The activation function for the output layer is a linear function. A summary of the most relevant parameters and methods is provided in Table 5.5.
With respect to the NN training, a mini-batch stochastic gradient descent (SGD) method was considered, with 200 batches and 1000 training epochs. The designed Neural Network provides good performance for the problem considered in this work, as we will show in the numerical results. However, a significant aspect in the performance fine-tuning of NN is the hyperparameter optimisation. A NN hyperparameters are the variables which determine the network structure (*e.g.*, the number of hidden layers or ac-

Table 5.5: *Hyperparameters of the Neural Network for the first (non-optimised) implementation.*

number of hidden layers	2
number of input nodes	22
number of output nodes	1
number of nodes in the hidden layers	11
activation function in the hidden layers	relu
activation function in the output layer	linear
learning optimizer	SGD
loss function	MSE
number of batches	200
number of epochs	1000

tivation functions) and the variables which determine how the network is trained (*e.g.*, the learning rate or the batch size). Each of these values can have a significant impact on the network performance, either in terms of convergence time or in terms of accuracy. One of the most common approaches to optimise and fine-tune the NN is to implement a grid search algorithm: for a subset (or, eventually, all of the) hyperparameters, instead of specifying the exact function or value, a range of possible options are provided. The NN is run and its performance evaluated for each possible combination of hyperparameters and the set of hyperparameters yielding to the best performance is selected. In this work, we considered the parameters for grid search as reported in Table 5.6, which also provides the selected hyperparameters. The objective function to be minimised by the NN is the Mean Squared Error (MSE). The MVP regression is applied with different degrees of the polynomial (P), in particular from $P = 1$ to $P = 5$. The higher the degree, the better is the accuracy on fitting the training set. However, when the model is applied to the test set in order make the prediction, the accuracy increases going from $P = 1$ to $P = 2$, but then it

Table 5.6: *Hyperparameters ranges and corresponding optimum values (in bold) for the optimisation of the Neural Network..*

number of nodes in the hidden layers	7, **8**, 9, 10, 11, 12
activation function in the hidden layers	softmax, elu, **relu**, linear, sigmoid
learning optimizer in the output layer	SGD, **Adam**, Adagrap
number of batches	20, 50, **100**, 200, 300

decreases at each additional degree of the polynomial (*i.e.*, with $P = 3$ it performs worse than with $P = 2$, with $P = 4$ it performs worse than $P = 3$, and so on). This behaviour is typically due to the overfitting. Ultimately, the best score with the MVP regression is obtained with the polynomial regression having $P = 2$ (MVP2). In the MVP, P is the only parameter that can be set, once the number of features has been fixed. The metric used to evaluate the performance is the R-squared value (also known as coefficient of determination), which is a typical metric associated to regression model performance. The same metric is used also for the NN, in order to make the comparison meaningful. As shown in Figure 5.9, the boosted NN provides the best (k-fold average) R-squared (0.98) among the considered regression models. The non-optimized NN also shows a good performance (0.91), although it is obtained with a fixed set up of the hyperparameters, *i.e.*, no optimisation procedure is performed. Figures 5.10a and 5.10b show the consumption (predicted vs simulated) when using a 2^{nd} order MVP or a NN regression, respectively. The points belong to one of the test sets randomly selected when applying the k-fold method. The identity function is also shown in the plots as a reference for the points. Figure 5.11 represents a time series extracted from the same set (the predicted values and the cor-

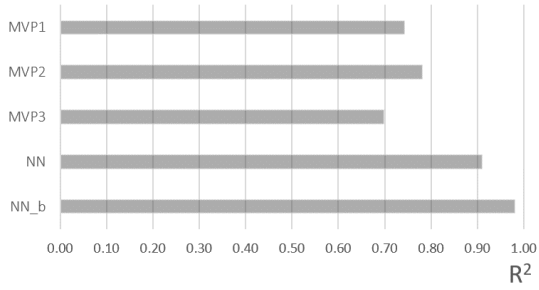

Figure 5.9: *Comparison of the performance of the regression models based on the R-squared metric for the considered Neural Network (NN) and Multivariate Polynomial Regression (MVP) approaches.*

responding simulated ones). The numerical results show that the NN-based method provides better performance in the energy consumption prediction, especially when the hyperparameters on the NN are optimised. Furthermore, this method avoids the overfitting issue, which is present when the MVP regression is applied (an issue arising in particular with polynomial degrees higher than 2). Having a prediction of the electric consumption in the near future is a key information that can be used in different control strategies aimed at pursuing a particular objective. For instance, the consumption could be minimised with an optimization algorithm in order to obtain the optimal set of control parameters (set-points). In a scenario in which the system is connected with a photovoltaic array (with/without battery), the objective function to be minimised could be the energy withdrawn from or delivered to the grid or, alternatively, a combination of these two quantities. The energy exchanges with the grid can be calculated having knowledge of the irradiance (forecast of n hours ahead) and electrical consumption (predicted, *e.g.*, with the method hereby presented).

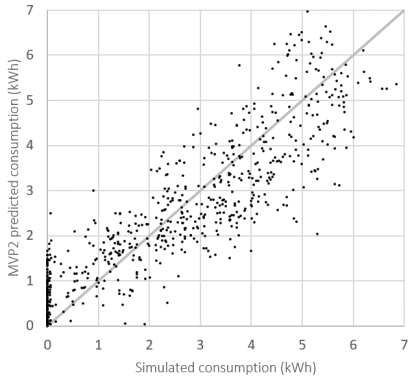

(a) *Consumption predicted by the 2nd order multivariate polynomial regression (MVP2) vs the consumption simulated with the dynamic model.*

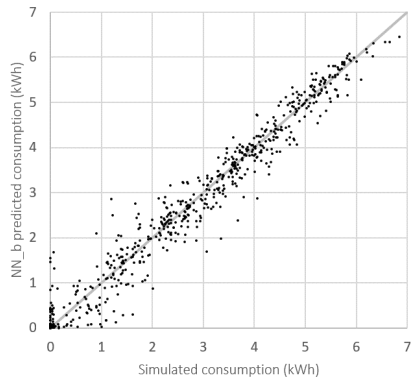

(b) *Consumption predicted by the boosted NN (NNb) vs the consumption simulated with the dynamic model.*

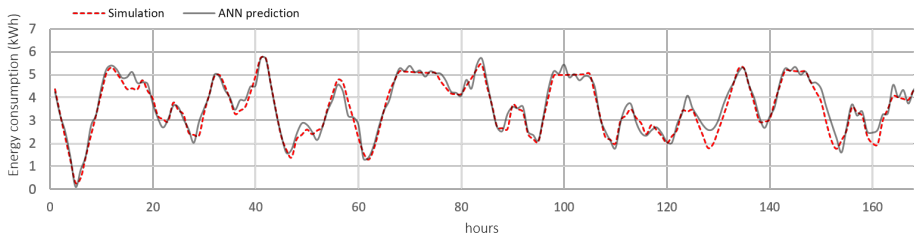

Figure 5.11: *Time series of electric energy consumption (integrals over 5 hours ahead): simulation vs prediction with boosted Neural Network.*

CHAPTER 6

Conclusions

Final comments

In the first part of the thesis, particular attention is pointed towards HP modelling, and, more specifically, on how it is possible to handle some issues that arise in implementing the HP control. Implementing the HP control externally to the HP model, which is directly controlled by a signal representing the compressor speed, results to have many advantages, including the versatility of the control strategy and an operation control that reflects the one implemented in real machines. Climate variables, such as temperature and radiation, strongly affect the behaviour of the analysed system, since they have a multiple influence on it. This work shows that, despite

the very different yearly distributions of solar radiation and heating/cooling needs across Europe, the capability to consume the self-produced energy on a yearly basis without any electrical storage (*i.e.*, the natural matching of load and radiation) does not significantly change for different climates. By adding a battery, the self-consumption increases in all the climates, but in the warmest ones it increases more, since, during winter months, the heating load occurs mainly during the night and it can be shifted by means of the electrical storage to match the daily radiation. The presence of a battery has an impact even greater on the self-sufficiency level for heating and cooling need, which is shown reaching values of 100%, with the battery and in warm climates. However, the electrical storage under the current cost scenario and without subsidies, is on average not profitable in terms of net present value, (Schopfer et al., 2018). Therefore, for increasing the self-consumption in cases where the initial cost of a battery is not affordable and/or profitable, other solutions have to be found. Control strategies aimed at improving the demand management by controlling the thermal storage are an effective and feasible solution. As shown in this work, the strategies aimed at increasing the self-consumption by exploiting the thermal capacity of the system yield to a higher SC ratio, although the increase is greatly influenced by the installed PV power. Algorithms based on both instantaneous values (PV production, external temperature) and weather forecast are applied. Pre-defined actions based on the near-future evolution of the weather have a limited applicability, unless the occupant's behaviour is also known in advance. For instance, waiting for the solar radiation in the morning in order to heat up the DHW, implies to know in advance that it will be a sunny morning, but also that the occupant's will not need hot water before a certain time. However, by means of machine learning algorithms and/or schedules defined by the occupant's themselves, these data

are not difficult to obtain. The analysed control strategies based on the near-future price evolution are mainly aimed at reducing the electricity bill for the households rather than improving energy performance indicators. However, when the variable price daily profile has the typical double-peak shape, exploiting the price reduction during the midday hours also yields to a higher HP performance (due to the warmer air temperature compared to the morning and evening hours). In a scenario without PV system, the proposed price-based algorithm has shown benefits only in case of marked peaks of the price during the day and in months with a continuous demand for heating. In scenarios with PV, the benefits are appreciable only if the priority is to maximize the self-consumption and the price-based function is applied secondly. In the last part of the thesis a machine learning technique (neural network, NN) is used to predict the electric energy consumption in a time interval of the near-future. The interest in predicting the building consumption started growing about a decade ago (Amasyali and El-Gohary, 2018) and it is still a very relevant topic (as demonstrated by (Zhao and Magoulès, 2012)) for different reasons, included the search for the optimal control of buildings. On the author's opinion, data-driven self-learning algorithms will play a key role in the control of buildings in the future, since rule-based solutions have to be studied *ad-hoc* for each system and this would imply a higher cost of the technology. The dynamic simulation will also be essential, especially in the design phase of a building and to test the good performance of control algorithms, before the actual installation.

Further work

As a continuation of the study presented in this thesis, further work on different aspects may be addressed. As for to the modelling part, it would be

interesting to calibrate the FC HP model presented in Chapter 2 with experimental data. A variable-speed air-to-water heat pump should be operated in a climatic chamber (with variable load emulator) or in a real application, for a sufficient variability of boundary conditions. However, among the analysed topics, the one with the highest potential for future developments is the control of the system. More specifically, control algorithms involving optimization (*e.g.*, model predictive control) and machine learning techniques (*artificial neural networks*) are receiving an ever increasing attention in the academic and industrial contexts. Although the basis for the implementation of these methods have been known for decades, there still are plenty of opportunities for their development and for their application in the context of energy management and control in buildings, which will be made possible through the deployment of telecommunications networks at building or district level, for an efficient and global control based on real-time information.

Bibliography

Amasyali K. and El-Gohary N. M. (2018), 'A review of data-driven building energy consumption prediction studies', *Renewable and Sustainable Energy Reviews* **81**, 1192–1205.

Arteconi A. (2018), 'An overview about criticalities in the modelling of multi-sector and multi-energy systems', *Environments* **5**, 1–10.

Arteconi A., Hewitt N. J. and Polonara F. (2013), 'Domestic demand-side management (dsm): Role of heat pumps and thermal energy storage (tes) systems', *Applied Thermal Engineering* **51**, 155–165.

Arteconi A., Mugnini A. and Polonara F. (2019), 'Energy flexible buildings: A methodology for rating the flexibility performance of buildings with electric heating and cooling systems', *Applied Energy* **251**, 1–17.

Arteconi A. and Polonara F. (2018), 'Assessing the demand side management potential and the energy flexibility of heat pumps in buildings', *Energies* **11**, 1–19.

Bacher P., Madsen H., Nielsen H. A. and Perers B. (2013), 'Short-term heat load forecasting for single family houses', *Energy and Buildings* **65**, 101–112.

Baggio P. (2013), Air to water heat pumps performance evaluation: a quick look at the relevant standards, *in* '30th AiCARR congress (Italian Association of Air Conditioning, Heating and Refrigeration); Innovazione e Tendenze nella Tecnologia e nelle Applicazioni delle Pompe di Calore'.

Bales C., Betak J., Broum M., Chèze D., Cuvillier G., Haberl R., Hafner B., Haller M. Y., Hamp Q., Heinz A., Hengel F., Kruck A., Matuska T., Mojic I., Petrak J., Poppi S., Sedlar J., Sourek B., Thissen B. and Weidinger A. (2015), *Optimized solar and heat pump systems, components and dimensioning*, Del. 7.3, MacSheep - New Materials and Control for a next generation of compact combined Solar and heat pump systems with boosted energetic and exergetic performance.

Beck T., Kondziella H., Huard G. and Bruckner T. (2017), 'Optimal operation, configuration and sizing of generation and storage technologies for residential heat pump systems in the spotlight of self-consumption of photovoltaic electricity', *Applied Energy* **188**, 604–619.

Biegel B., Andersen P., Pedersen T. S., Nielsen K. M., Stoustrup J. and Hansen L. H. (2013), Electricity market optimization of heat pump portfolio., *in* 'Proceedings of the IEEE international conference on control applications (CCA)', pp. 294–301.

Chua K. J., Chou S. K. and Yang W. M. (2010), 'Advances in heat pump systems: A review', *Applied Energy* **87**(12), 3611–3624.

Clauß J., Stinner A., Sartori I. and Georges L. (2019), 'Predictive rule-based control to activate the energy flexibility of norwegian residential buildings: Case of an air-source heat pump and direct electric heating', *Applied Energy* **237**, 500–518.

Coccia G., Arteconi A., D'Agaro P., Polonara F. and Cortella G. (2018), 'Demand side management analysis of a commercial water loop heat pump system', *Modelling, Measurement and Control C* **79**, 111–118.

Crawley D. B. (1998), 'Which weather data should you use for energy simulations of commercial buildings?', *Transactions-American society of heating refrigerating and air conditioning engineers* **104**, 498–515.

CTI (2015), *Test reference years for thermotechnical applications*, https://try.cti2000.it.

Daut M. A. M., Hassan M. Y., Abdullah H., Rahman H. A., Abdullah M. P. and Hussin F. (2017), 'Building electrical energy consumption forecasting analysis using conventional and artificial intelligence methods: A review', *Renewable and Sustainable Energy Reviews* **70**, 1108–1118.

De Coninck R., Baetens R., Saelens D., Woyte A. and Helsen L. (2014), 'Rule-based demand-side management of domestic hot water production with heat pumps in zero energy neighbourhoods', *Journal of Building Performance Simulation* **7**, 271–288.

De Soto W., Klein S. A. and Beckman W. A. (2006), 'Improvement and validation of a model for photovoltaic array performance', *Solar Energy* **80**, 78–88.

D'hulst R., Labeeuw W., Beusen B., Claessens S., Deconinck G. and Vanthournout K. (2015), 'Demand response flexibility and flexibility potential of residential smart appliances: Experiences from large pilot test in belgium', *Applied Energy* **155**, 79–90.

Di Perna C., Stazi F., Ursini Casalena A. and D'Orazio M. (2011), 'Influence of the internal inertia of the building envelope on summertime comfort in

buildings with high internal heat loads', *Energy and Buildings* **43**, 200–206.

Dong B., Yan D., Li Z., Jin Y., Feng X. and Fontenot H. (2018), 'Modeling occupancy and behavior for better building design and operation—a critical review', *Building Simulation* **11**, 899–921.

Dongellini M., Naldi C. and Morini G. L. (2015), 'Seasonal performance evaluation of electric air-to water heat pump systems', *Applied Thermal Engineering* **90**, 1072–1081.

ENEA (2011), *Definizione degli anni tipo climatici delle province delle regioni italiane del centro sud*, Report RdS/2011/9 Agenzia Nazionale per le Nuove Tecnologie, l'Energia e lo Sviluppo Economico Sostenibile.

ENEA (2012), *Aggiornamento parametri climatici nazionali e zonizzazione del clima nazionale ai fini della certificazione estiva*, Report RdS/2012/106 Agenzia Nazionale per le Nuove Tecnologie, l'Energia e lo Sviluppo Economico Sostenibile.

Enerdata (2008), *Average floor area per capita*, http://www.entranze.enerdata.eu.

Esser A. and Sensfuss F. (2016), *Review of the default primary energy factor (PEF) reflecting the estimated average EU generation efficiency referred to in Annex IV of Directive 2012/27/EU and possible extension of the approach to other energy carriers*, Final report - Evaluation of primary energy factor calculation options for electricity.

European Commission (2007), *Energy performance of buildings - Economic evaluation procedure for energy systems in buildings*, EN 15459:2007.

European Commission (2008), *Heating systems in buildings - Method for calculation of system energy requirements and system efficiencies - Part 4-2: Space heating generation systems, heat pump systems*, UNI EN 15316-4-2:2008.

European Commission (2009), *Directive 2009/28/EC of the European Parliament and of the Council of 23 April 2009 on the promotion of the use of energy from renewable sources and amending and subsequently repealing Directives 2001/77/EC and 2003/30/EC*, Directive 2009/28/EC.

European Commission (2016), *Air conditioners, liquid chilling packages and heat pumps, with electrically driven compressors, for space heating and cooling - Testing and rating at part load conditions and calculation of seasonal performance*, EN 14825:2016.

European Commission (2017), *Energy performance of buildings - Method for calculation of the design heat load - Part 3: Domestic hot water systems heat load and characterisation of needs, Module M8-2, M8-3*, EN 12831-3:2017.

European Heat Pump Agency (2015), *European Heat Pump Market and Statistics Report 2015*.

European Heat Pump Agency (2018), *Overview - Renewable energy created by stock of heat pumps, in TWh*, http://www.stats.ehpa.org/.

European Union (2010), *Directive 2010/31/EU of the European Parliament and of the Council of 19 May 2010 on the energy performance of buildings*, Directive 2010/31/EU.

European Union (2012), *Directive 2012/27/EU of the European Parliament and of the Council of 25 October 2012 on energy efficiency, amending Directives 2009/125/EC and 2010/30/EU and repealing Directives 2004/8/EC and 2006/32/EC*, Directive 2012/27/EU.

eurostat (2018), *Electricity price statistics*, https://ec.europa.eu/eurostat/statistics-explained/ accessed on March 6, 2019.

Fabrizio E., Seguro F. and Filippi M. (2014), 'Integrated hvac and dhw production systems for zero energy buildings', *Renewable and Sustainable Energy Reviews* **40**, 515–541.

Facci A. L., Krastev V. K., Falcucci G. and Ubertini S. (2018), 'Smart integration of photovoltaic production, heat pump and thermal energy storage in residential applications', *Solar Energy* pp. 1–11.

Fischer D., Bernhardt J., Madani H. and Wittwer C. (2017), 'Comparison of control approaches for variable speed air source heat pumps considering time variable electricity prices and pv', *Applied Energy* **204**, 93–105.

Fischer D., Lindberg K. B., Madani H. and Wittwer C. (2016), 'Impact of pv and variable prices on optimal system sizing for heat pumps and thermal storage', *Energy and Buildings* **128**, 723–733.

Fischer D. and Madani H. (2017), 'On heat pumps in smart grids: A review. renewable and sustainable energy reviews', *Renewable and Sustainable Energy Reviews* **70**, 342–357.

Fischer D., Rautenberg F., Wirtz T., Wille-Haussmann B. and Madani H. (2015), Smart meter enabled control for variable speed heat pumps to

increase pv self-consumption, *in* 'Proceedings of the 24th International Congress on Refrigeration (ICR)'.

Goia F., Time B. and Gustavsen A. (2015), 'Impact of opaque building envelope configuration on the heating and cooling energy need of a single family house in cold climates', *Energy Procedia* **78**, 2626–2631.

Goodfeloow I., Bengio Y. and Courville A. (2016), *Deep Learning*, MIT Press.

Harkouss F., Fardoun F. and Biwole P. H. (2018), 'Optimization approaches and climates investigations in nzeb—a review', *Building Simulation* **11**, 923–952.

Henze G. P., Felsmann C. and Knabe G. (2004), 'Evaluation of optimal control for active and passive building thermal storage', *International Journal of Thermal Sciences* **43**(2), 173–183.

International Energy Agency (2019), *Heating in buildings - Tracking Clean Energy Progress.*

International Weather for Energy Calculations (n.d.), *ASHRAE International Weather Files for Energy Calculations 2.0 (IWEC2)*, https://www.ashrae.org/technical-resources/.

Jordan U. and Vajen K. (2005), Dhwcalc: Program to generate domestic hot water profiles with statistical means for user defined conditions, *in* 'ISES Solar World Congress'.

Junker R. G., Azar A. G., Lopes R. A., Lindberg K. B., Reynders G., Relan R. and Madsen H. (2018), 'Characterizing the energy flexibility of buildings and districts', *Applied Energy* **225**, 175–182.

Leppin L. (2017), 'Development of operational strategies for a heating pump system with photovoltaic, electrical and thermal storage', *Master Level Thesis European Solar Engineering School* .

Luthander R., Widén J., Nilsson D. and Palm J. (2015), 'Photovoltaic self-consumption in buildings: A review', *Applied Energy* **142**, 80–94.

Masy G., Georges E., Verhelst C., Lemort V. and André P. (2015), 'Smart grid energy flexible buildings through the use of heat pumps and building thermal mass as energy storage in the belgian context', *Science and Technology for the Built Environment* **21**, 800–811.

Naldi C., Dongellini M., Morini G. L. and Zanchini. E. (2015), Comparison between hourly simulation and bin-method for the seasonal performance evaluation of electric air-source heat pumps for heating, *in* 'Building Simulation Applications 2015 - 2nd IBPSA-Italy Conference'.

Pallonetto F., Oxizidis S., Milano F. and Finn D. (2016), 'The effect of time-of-use tariffs on the demand response flexibility of an all-electric smart-grid-ready dwelling', *Energy and Buildings* **128**, 56–67.

Patteeuw D., Henze G. P. and Helsen L. (2016), 'Comparison of load shifting incentives for low-energy buildings with heat pumps to attain grid flexibility benefits', *Applied Energy* **167**, 80–92.

Péan T. Q., Salom J. and Costa-Castelló R. (2019), 'Review of control strategies for improving the energy flexibility provided by heat pump systems in buildings. journal of process control', *Journal of Process Control* **74**, 35–49.

Penna P., Prada A., Cappelletti F. and Gasparella A. (2015), 'Multi-objectives optimization of energy efficiency measures in existing buildings', *Energy and Buildings* **95**, 57–69.

Persson T. and Heier J. (2010), 'Småhusens framtida utformning: -Hur påverkar Boverkets nya byggregler?', *Region Gävleborg, Gävle* .

PV Magazine (2019), *Module Price Index*, https://www.pv-magazine.com/features/investors/module-price-index/.

Raza M. and Khosravi A. (2015), 'A review on artificial intelligence based load demand forecasting techniques for smart grid and buildings', *Renewable and Sustainable Energy Reviews* **50**, 1352–1372.

Reynders G., Nuytten T. and Saelens D. (2013), 'Potential of structural thermal mass for demand-side management in dwellings', *Building and Environment* **64**, 187–199.

Rodriguez R. L., Ramos S., Álvarez Dominguez J. and Eicker U. (2018), 'Contributions of heat pumps to demand response: A case study of a plus-energy dwelling', *Applied Energy* **214**, 191–204.

Salpakari J. and Lund P. (2016), 'Optimal and rule-based control strategies for energy flexibility in buildings with pv', *Applied Energy* **161**, 425–436.

Schibuola L., Scarpa M. and Tambani C. (2015), 'Demand response management by means of heat pumps controlled via real time pricing', *Energy and Buildings* **90**, 15–28.

Schopfer S., Tiefenbeck V. and Staake T. (2018), 'Economic assessment of photovoltaic battery systems based on household load profiles', *Applied Energy* **223**, 229–248.

Shibata Y. (2011), 'Aerothermal energy use by heat pumps in japan', *The Institute of Energy Economics* pp. 1–13.

Swedish Energy Agency (2018), *Electric energy price agreements Sweden 2013-2016*, http://www.scb.se/en/finding-statistics/statistics-by-subject-area/energy/price-trends-in-the-energy-sector/prices-on-electricity-and-transmission-of-electricity-network-tariffs.

Tam A., Ziviani D., Braun J. E. and Jain N. (2019), 'Development and evaluation of a generalized rule-based control strategy for residential ice storage systems', *Energy and Buildings* **197**, 99–111.

Thygesen R. and Karlsson B. (2016), 'Simulation of a proposed novel weather forecast control for ground source heat pumps as a mean to evaluate the feasibility of forecast controls' influence on the photovoltaic electricity self-consumption', *Applied Energy* **164**, 579–589.

Tian W., Heo Y., de Wilde P., Li Z., Yan D., Park C. S., Feng X. and Augenbroe G. (2018), 'A review of uncertainty analysis in building energy assessment', *Renewable and Sustainable Energy Reviews* **93**, 285–301.

UNI (2016*a*), *Energy performance of buildings - Part 1: Evaluation of energy need for space heating and cooling*, UNI/TS 11300-1:2014.

UNI (2016*b*), *Energy performance of buildings - Part 4: Renewable energy and other generation systems for space heating and domestic hot water production*, UNI/TS 11300-4:2016.

Uytterhoeven A., Arteconi A. and Helsen L. (2019), Decentralised storage and demand response: impact on renewable share in grids and buildings, *in* 'World Sustainable Energy Days (WSED), Wels, Austria'.

Widén J. (2014), 'Improved photovoltaic self-consumption with appliance scheduling in 200 single-family buildings', *Applied Energy* **126**, 199–212.

Widén J. and Wäckelgård E. (2010), 'A high-resolution stochastic model of domestic activity patterns and electricity demand', *Applied Energy* **87**, 1880–1892.

Williams C. J. C., Binder J. O. and Kelm T. (2012), Demand side management through heat pumps, thermal storage and battery storage to increase local self-consumption and grid compatibility of pv systems, *in* '2012 3rd IEEE PES Innovative Smart Grid Technologies Europe (ISGT Europe)'.

Zhang Y., Lundblad A., Campana P. E., Benavente F. and Jinyue Y. (2017), 'Battery sizing and rule-based operation of grid-connected photovoltaic-battery system: A case study in sweden', *Energy Conversion and Management* **133**, 249–263.

Zhao H.-X. and Magoulès F. (2012), 'A review on the prediction of building energy consumption', *Renewable and Sustainable Energy Reviews* **16**, 3586–3592.

Zhou Q., Wang S., Xu X. and Xiao F. (2008), 'A grey-box model of next-day building thermal load prediction for energy-efficient control', *International Journal of Energy Research* **32**, 1418–1431.